New Phytologist

Research

Arabidopsis thaliana rosette habit is controlled by combined light and energy signaling converging on transcriptional control of the TALE homeobox gene *ATH1*

Shahram Shokrian Hajibehzad[1,2], Savani S. Silva[1], Niels Peeters[1], Evelien Stouten[1], Guido Buijs[1], Sjef Smeekens[1] and Marcel Proveniers[1,2]

[1]Molecular Plant Physiology, Department of Biology, Science4Life, Utrecht University, Padualaan 8, Utrecht, 3584 CH, the Netherlands; [2]Translational Plant Biology, Department of Biology, Science4Life, Utrecht University, Padualaan 8, Utrecht, 3584 CH, the Netherlands

Author for correspondence:
Marcel Proveniers
Email: m.proveniers@uu.nl

Received: *23 February 2023*
Accepted: *3 May 2023*

New Phytologist (2023) **239:** 1051–1067
doi: 10.1111/nph.19014

Key words: *ARABIDOPSIS THALIANA* HOMEOBOX 1 (ATH1), internode development, meristem activity, photomorphogenesis, rosette habit, TOR kinase.

Summary

- In the absence of light signals, Arabidopsis plants fail to develop the rosette habit typical for this species. Instead, plants display caulescent growth due to elongation of rosette internodes. This aspect of photomorphogenic development has been paid little attention and molecular events involved, downstream of photoreceptor signaling, remain to be identified.
- Using a combination of genetic and molecular approaches, we show that Arabidopsis rosette habit is a photomorphogenic trait controlled by induction of *ARABIDOPSIS THALIANA HOMEOBOX GENE1* (*ATH1*) as downstream target of multiple photoreceptors.
- *ATH1* induction prevents rosette internode elongation by maintaining the shoot apical meristem (SAM) rib zone area inactive and requires inactivation of photomorphogenesis inhibitors, including PHYTOCHROME INTERACTING FACTOR (PIF) proteins. *ATH1* activity results in tissue-specific inhibition of *PIF* expression, establishing double-negative feedback-regulation at the SAM. Light-requirement for *ATH1* expression can be overcome by high sugar availability to the SAM. Both sugar and light signals that induce *ATH1* and, subsequently, rosette habit are mediated by TOR kinase.
- Collectively, our data reveal a SAM-specific, double-negative ATH1-PIF feedback loop at the basis of rosette habit. Upstream, TOR kinase functions as central hub integrating light and energy signals that control this for Arabidopsis quintessential trait.

Introduction

Plants are equipped with sophisticated mechanisms to sense the environment and to adapt their growth and development accordingly. Being photoautotrophs, plants are especially attuned to the light environment. This is well-illustrated by the dramatic differences in appearance between light- and dark-grown seedlings. In Arabidopsis, dark-grown seedlings have a typical etiolated phenotype, characterized by an elongated hypocotyl, apical hook formation, closed cotyledons, and an arrested shoot apical meristem (SAM). Exposure to light results in inhibition of hypocotyl elongation, apical hook opening, opening and expansion of cotyledons, and SAM activation (Chen & Chory, 2011; Pfeiffer *et al.*, 2016; Mohammed *et al.*, 2017; Janocha *et al.*, 2021). The active SAM gives rise to the aerial plant structures. During the vegetative phase, leaf primordia arise in a spiral phyllotaxy to form a basal rosette in which internode elongation remains arrested. In the absence of light, SAM activity can be induced by exposing the SAM to metabolizable sugar, such as sucrose (Araki & Komeda, 1993; Roldán *et al.*, 1999). Both light- and sugar-mediated SAM activation involve TARGET OF RAPAMYCIN (TOR) kinase, a central component in energy sensing, such that it promotes SAM activity in favorable conditions (Pfeiffer *et al.*, 2016; Li *et al.*, 2017; Mohammed *et al.*, 2017; Janocha *et al.*, 2021). It has been proposed that light, via photoreceptor signaling through CONSTITUTIVE PHOTOMORPHOGENIC1 (COP1), plays a permissive role toward energy signaling in the SAM, possibly by controlling sugar import into the meristem (Mohammed *et al.*, 2017). This might explain why direct access of the SAM to metabolizable sugar can activate the meristem in the absence of light.

Sugar-induced dark morphogenesis in Arabidopsis follows the same developmental phases as in light-grown plants. However, contrary to light-grown plants, in sugar-induced plants, stem elongation is not inhibited during vegetative development. Consequently, such plants fail to display a rosette habit and elongated internodes are present between adjacent 'rosette' leaves (Roldán *et al.*, 1999; Mohammed *et al.*, 2017). Similar loss of rosette habit has been observed in light-grown plants lacking several phytochrome (phy) and/or cryptochrome (CRY) photoreceptors (Devlin *et al.*, 1996, 1998, 1999, 2003; Whitelam & Devlin, 1997; Whitelam *et al.*, 1998; Roldán *et al.*, 1999; Mazzella

et al., 2000; Franklin *et al.*, 2003; Hu *et al.*, 2013). In addition, ambient temperature has been reported to modulate light-regulation of rosette habit. At elevated ambient temperature, phyB and CRY1 redundantly suppress elongation of vegetative internodes (Mazzella *et al.*, 2000). A compact rosette habit thus is a *bona fide* photomorphogenic trait in Arabidopsis. However, despite numerous observations and the economic importance of rosette habit in vegetable crops, this aspect of photomorphogenic development has been paid little attention and molecular events involved downstream of photoreceptor signaling remain to be identified.

In Arabidopsis, internode elongation reflects the activity of the basal part of the SAM, the rib zone (RZ). In light-grown plants, the RZ is compact and mitotically inactive during vegetative growth, resulting in the formation of a compact rosette. At floral transition, the RZ becomes activated to provide cells for rapid elongation of inflorescence internodes of the inflorescence stem (Vaughan, 1955; Sachs *et al.*, 1959; Peterson & Yeung, 1972; Jacqmard *et al.*, 2003; Bencivenga *et al.*, 2016; Serrano-Mislata *et al.*, 2017). Previously, ectopic expression of *ARABIDOPSIS THALIANA HOMEOBOX GENE1* (*ATH1*) was shown to suppress growth of the inflorescence stem, due to inhibition of internode elongation (Cole *et al.*, 2006; Gómez-Mena & Sablowski, 2008; Rutjens *et al.*, 2009; Ejaz *et al.*, 2021). In wild-type plants, *ATH1* is expressed at the vegetative SAM. At floral transition, when stem growth is initiated, *ATH1* is rapidly downregulated. In plants lacking functional ATH1, the subapical region, where the RZ is located, is enlarged during vegetative development, suggesting that ATH1 restricts growth of this part of the SAM (Proveniers *et al.*, 2007; Gómez-Mena & Sablowski, 2008). In line with this, light-grown *ath1* mutants display slightly elongated rosette internodes, resembling those of higher order photoreceptor mutants (Li *et al.*, 2012; Ejaz *et al.*, 2021). *ATH1* was originally identified in a screen for light-regulated genes and its expression is induced by light during seedling de-etiolation (Quaedvlieg *et al.*, 1995). In dark-grown seedlings lacking COP1, *ATH1* transcript levels are elevated as well, suggesting that *ATH1* expression is under the control of this negative regulator of photomorphogenesis (Quaedvlieg *et al.*, 1995; Proveniers *et al.*, 2007). In line with this, *cop1* mutants exhibit a constitutive deetiolated phenotype in darkness, including formation of a compact rosette (Deng & Quail, 1992). Together with SUPPRESSOR OF PHYA-105 (SPA) proteins, COP1 forms an E3 ubiquitin ligase complex, which acts by regulating the stability of photomorphogenesis-promoting transcription factors. In addition, COP1/SPA stabilizes proteins of the PHYTOCHROME INTERACTING FACTOR (PIF) family in darkness to promote etiolation (Ponnu & Hoecker, 2021). Upon exposure to light, phytochromes physically interact with PIF proteins and promote their turnover, resulting in de-etiolation (Pham *et al.*, 2018a; Ponnu & Hoecker, 2021).

Here, we show that ATH1 confers rosette habit in light-grown, vegetative Arabidopsis plants by integration of signals from multiple photoreceptors. *ATH1* is induced by blue, red, and far-red light requiring both PHY- and CRY-family photoreceptors. Dark-grown wild-type plants, and higher order photoreceptor mutants display strongly reduced levels of *ATH1* in the SAM. In both cases, increased expression of *ATH1* is sufficient to restore compact rosette internodes. Finally, we introduce a regulatory feedback loop whereby multiple PIFs and ATH1 repress each other's expression in a tissue-specific manner, contributing to the maintenance of rosette habit.

Furthermore, in the absence of light, *ATH1* can be induced by the direct availability of metabolic sugars to the SAM. We show that increasing amounts of sucrose result in a corresponding increase in *ATH1* expression and associated increased inhibition of vegetative internode elongation. Both light- and metabolic signal-mediated induction of *ATH1* at the SAM requires activation of TOR kinase.

Materials and Methods

Plant materials and growth conditions

Arabidopsis thaliana (L.) Heynh. seeds were obtained from the Nottingham Arabidopsis Stock Center (http://arabidopsis.info/) or were kind gifts. For genotypes used, see Supporting Information Table S1.

ATH1$_{pro}$:GUS-containing lines were obtained through crosses. Offspring was backcrossed at least four times to parental acceptor genotypes. *Pro$_{35S}$:HA-ATH1*-containing lines were obtained through genetic transformation as described previously (Proveniers *et al.*, 2007). Per genotype over 10 independent, homozygous single insert lines were used for further analysis. To obtain *cop1-4 ath1-4* and *pifq ath1-3* plants, F2 offspring from respective crosses was first phenotype-selected (*cop1-4*: short hypocotyl in darkness; *pifq*: short-petiole phenotype). Plants were then genotyped using primers listed in Table S2.

For plant growth, seeds were chlorine-gas sterilized for 4 h using a 4 ml 37% HCl/100 ml commercial bleach (4.5% active chlorine) mixture and put on soil (Primasta B.V., Asten, The Netherlands) or sterile 0.8% plant agar (Duchefa Biochemie B.V., Haarlem, The Netherlands) with full-strength Murashige–Skoog medium (MS salts including MES (pH 5.8) and vitamins; Duchefa Biochemie) in square Petri dishes (120 × 120 mm). After stratification (2–3 d, 4°C), plants were grown in climate-controlled growth cabinets (Microclima 1000; Snijders Labs, Tilburg, The Netherlands) in short-day (SD; 8 h : 16 h, light : dark) or long-day (LD; 16 h : 8 h, light : dark) photoperiods, under 120 μmol m^{-2} s^{-1} fluorescent white-light conditions (Luxline Plus Cool White, Sylvania, OH, USA) and 70% relative humidity. For monochromatic light conditions, a Snijders Microclima cabinet equipped with Philips GreenPower LEDs (red light: 124.35 μmol m^{-2} s^{-1}, blue light: 6.14 μmol m^{-2} s^{-1}, far-red light: 77.57 μmol m^{-2} s^{-1}) was used.

For liquid culture, 10–20 seeds were added to 20 ml of half-strength MS medium (MS salts including MES Buffer (pH 5.8) and vitamins; Duchefa Biochemie) in 100-ml bottles on a rotary shaker (185 rpm, 22°C). Bottles were sealed with Steristoppers® (Heinz Herenz, Hamburg, Germany). After stratification, seeds were exposed to fluorescent light (1–1.5 h, 120 μmol m^{-2} s^{-1}) to stimulate germination. Bottles were then wrapped in aluminum foil. Sucrose (50% w/v) or sorbitol (50% w/v) was added at the

start or day three of the experiment. To prevent seedling exposure to light, sugars were added by injection through the aluminum foil-covered bottle stopper using a syringe with long needle.

Ethanol-induction of TOR RNAi lines was previously described (Deprost *et al.*, 2007). Instead of growing plants on soil and using ethanol vapor for induction of the ethanol switch, plants were grown in liquid medium and, using syringe and needle, ethanol was added directly to the growth medium to a final concentration of 0.1% (v/v) after 5 d of dark cultivation. After an additional 5 h in darkness, sucrose was added. Plants were sampled after two more days of growth in darkness.

Growth in a CO_2-deficient environment was accomplished as in Pfeiffer *et al.* (2016).

Phenotypic analyses

For light-grown plants, total rosette internode length was measured using a caliper. For dark-grown seedlings, plants were photographed after 3 wk of growth and ImageJ (Schneider *et al.*, 2012) was used to measure total rosette internode length. Average rosette internode length was determined by dividing total rosette internode length by the total number of rosette leaves.

Meristem cell size was determined using confocal laser scanning microscopy. In median, longitudinal optical sections through shoot apices a central cell file extending from the epidermis into the subapical region where the hypocotyl vascular strands converge was identified. Using ImageJ, per position individual cell lengths were then measured in apical-basal direction.

Gene expression analysis

Samples were snap-frozen in liquid nitrogen and stored at −80°C before RNA extraction. For each experiment, three or four biological replicates and two technical replicates were included. RNA was isolated using a RNeasy mini or micro kit (Qiagen). Genomic DNA was removed using DNaseI (Thermo Fisher Scientific, Bleiswijk, The Netherlands) and cDNA was synthesized from 500 ng–1 µg RNA using RevertAid H Minus Reverse Transcriptase and Ribolock RNAse inhibitor (Thermo Fisher Scientific) and a mix of anchored odT(20) primers (Jena Bioscience, Jena, Germany) and random hexamers (IDT). qPCR reactions were performed using qPCRBIO SyGreen Blue mix (PCRBIO) on a ViiA7 Real Time PCR system. ViiA7 software was used to analyze the data. Relative expression levels were calculated using the ΔΔCt method (Livak & Schmittgen, 2001), normalized to *GAPC2* (AT1G13440) and/or *MUSE3* (AT5G15400) expression. For primer sequences used, see Table S3.

β-glucuronidase staining and microscopy

Seedlings were harvested and vacuum-infiltrated in β-glucuronidase (GUS) staining buffer (50 mM sodium phosphate buffer (pH = 7.2), supplemented with 0.1% Triton X-100, 100 mM, potassium ferrocyanide, 100 mM, potassium ferricyanide, 2 mM 5-bromo-4-chloro-3-indolyl glucuronide). Samples were incubated o/n at room temperature and subsequently cleared in ethanol. Images were taken with a Nikon DXMI200 camera attached to a Zeiss Stemi SV11 stereo microscope. GUS staining area was measured and quantified using ImageJ.

Confocal microscopy

Seedlings were cleared using the ClearSee method (Kurihara *et al.*, 2015) and imaged at a resolution of 0.25 × 0.25 × 0.5 µm using a Carl Zeiss LSM880 Fast AiryScan microscope with a Plan-Apochromat 63×/1.2 Imm Korr DIC objective (numerical aperture 1.40, oil immersion) and ZEN software (blue edition, Carl Zeiss). Calcofluor White Stain (Sigma-Aldrich) staining was performed as described before (Ursache *et al.*, 2018). Excitation was at 405 nm, and emission filters were set between 425 and 475 nm. All replicate images were acquired using identical microscopy parameters for each experiment. Images were processed with Fiji (v.1.52, Fiji) and Adobe Illustrator.

Statistical analysis

Data plotting and statistical analysis were performed using Rstudio.1.0.143 (www.rstudio.com) with R v.3.6.2 (https://cran.r-project.org/). To compare differences between experimental groups, one-way ANOVA and Fisher's Least Significant Difference test were applied. Before conducting ANOVA, the normality and homogeneity of variance assumptions were verified using histograms, ggnorm, and Shapiro tests for normality and the Levene and Bartlett tests for homogeneity. In cases where ANOVA assumptions were not met, the Dunn Test with the Benjamini–Hochberg method was used for multiple comparisons. *T*-tests were applied only if the assumptions were met for comparing two groups, otherwise the Kruskal–Wallis test was used. Results were corrected using the Bonferroni correction with an alpha level of 0.05, and all analyses were performed using the agricolae package (de Mendiburu, 2021). Figures were compiled using Adobe Illustrator and ImageJ software.

Results

ATH1 restores rosette habit in dark-grown plants

When germinated and grown in darkness stem cells remain dormant in Arabidopsis (Pfeiffer *et al.*, 2016; Mohammed *et al.*, 2017). This morphogenetic arrest can be overcome by availability of sucrose to the aerial part of the plant. Sugar-induced, dark-morphogenesis of Arabidopsis plants follows the same developmental phases as light-grown plants. However, such plants fail to develop a compact rosette (Fig. 1a,b). The compact rosette habit of light-grown Arabidopsis plants is conferred by ATH1 (Li *et al.*, 2012; Ejaz *et al.*, 2021). We tested whether *ATH1* expression is sufficient for the development of a compact rosette in dark-grown plants. For this, dexamethasone (Dex)-inducible *35Spro:ATH1-HBD* seedlings were grown in continuous darkness in the presence of sucrose (Fig. 1a,b). Induction of nuclear expression of ATH1 resulted in strong repression of rosette internode elongation and, consequently, restoration of

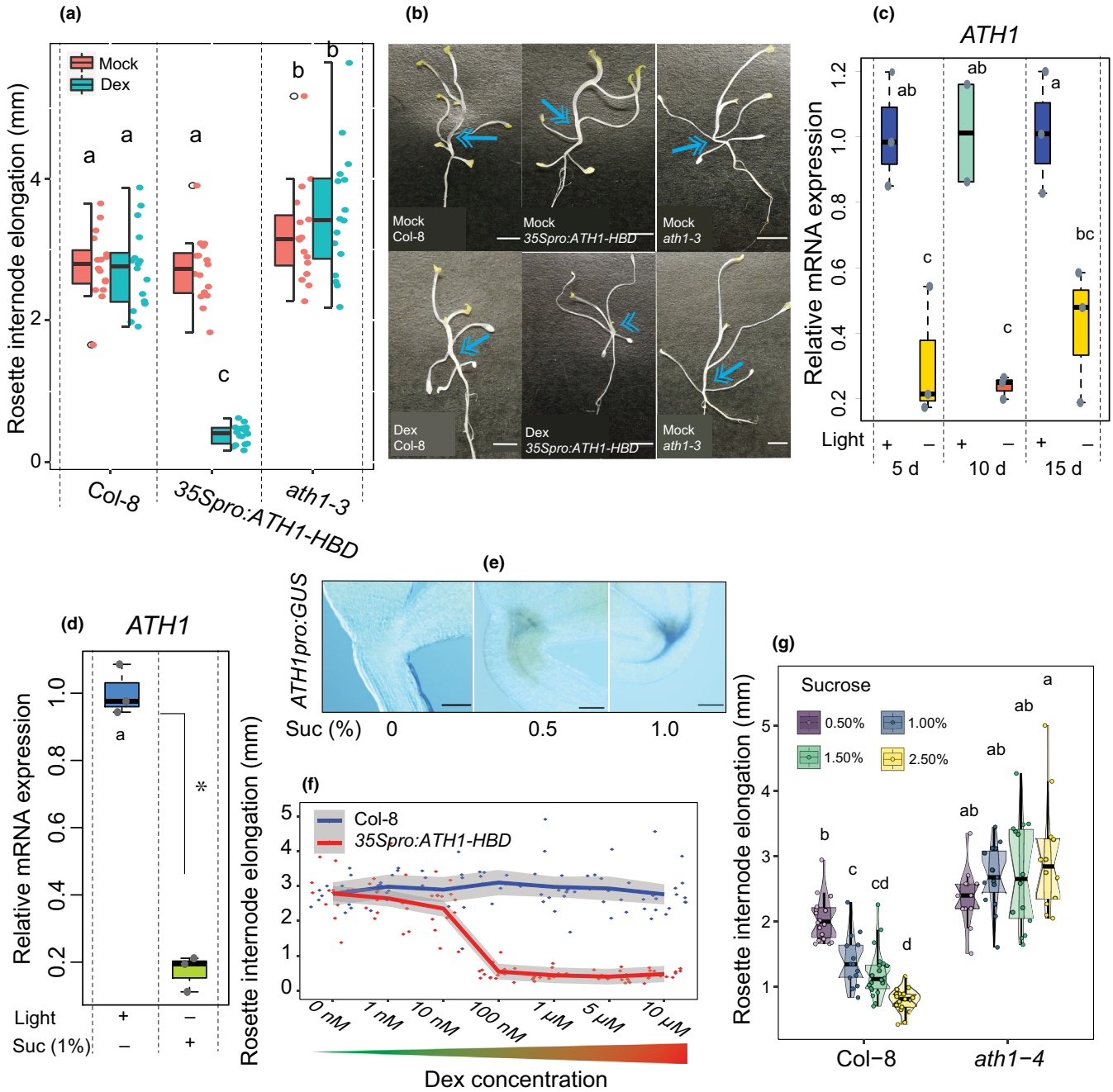

Fig. 1 *ARABIDOPSIS THALIANA HOMEOBOX GENE1* (*ATH1*) expression is sufficient to restore compact rosette growth in dark-grown *Arabidopsis thaliana* plants. (a) Average rosette internode elongation in dark-grown Col-8, *ath1-3*, and *35Spro:ATH1-HBD* plants treated with 0.1% ethanol (mock) or 10 μM dexamethasone (Dex). Sucrose was added 3 d after the start of the experiment. (b) Representative 3-wk-old, dark-grown plants used in (a). Arrows indicate elongated rosette internodes, the arrowhead indicates suppression of internode elongation. Bars, 2 mm. (c) Relative expression of *ATH1* in Col-8 plants grown for either 5, 10, or 15 d (d) in continuous light or continuous darkness at 22°C. Sucrose was present at a 1% final concentration from the beginning of the experiment. Transcript levels were normalized to *MUSE3* (AT5G15400). The average of three biological replicates is shown. Error bars represent SD of the ΔC_T mean. (d) Relative expression of *ATH1* in 7-d-old seedlings grown in continuous light (+) or continuous darkness (−) in the presence (+) or absence (−) of 1% sucrose. Transcript levels were normalized to *GAPC2* (AT1G13440). The average of three biological replicates is shown. The asterisk (*) in the figure represents a *P*-value of 0.04953 for the observed difference, determined using the non-parametric Kruskal–Wallis rank sum test. (e) β-glucuronidase (GUS)-stained 7-d-old, dark-grown $ATH1_{pro}$:*GUS* seedlings in the absence (0%) or presence (0.5% and 1%) of sucrose. GUS activity is visible as a blue precipitate. Bars, 0.01 mm. (f) Average rosette internode elongation in 3-wk-old dark-grown Col-8 and *35Spro:ATH1-HBD* plants treated with increasing concentrations of Dex (0 nM to 10 μM). The shaded areas around the lines represent the 95% confidence intervals. (g) Average rosette internode elongation of 3-wk-old dark-grown Col-8 and *ath1-4* seedlings treated with increasing concentrations of sucrose (0.5–2.5%). In (a, c, g) differing letters signify statistically significant differences ($P < 0.05$) as determined by a one-way analysis of variance with Tukey's honest significant difference *post hoc* test for (a, b), and a multiple comparison analysis using the Dunn Test with the Benjamini–Hochberg method for (g). In (a, f, g) colored dots indicate rosette internode elongation scores of individual seedlings. In boxplots (a, c, d) and violin plots (g), the center bar indicates median values, box edges correspond to interquartile ranges (IQR), and error bars display values within 1.5× IQR, with circular points as outliers. Violin plot width represents data density at specific values.

rosette habit, while Col-8 control plants and mock-treated *35Spro:ATH1-HBD* plants displayed elongated vegetative internodes, resulting in loss of rosette habit (Fig. 1a,b). Under these conditions, vegetative internodes of *ath1* mutants were slightly more elongated than those of control plants (Figs 1a,b, S1), suggesting that *ATH1* might still be expressed to some extent in the absence of light, despite previous findings showing otherwise (Quaedvlieg *et al.*, 1995). Possibly, sucrose addition to induce dark morphogenesis resulted in *ATH1* induction. Indeed, in the absence of both sucrose and light, *ATH1* was not expressed, whereas in the presence of 1% sucrose, *ATH1* transcript levels reached up to 20% of those in light-grown plants (Fig. 1c,d). Thus, sucrose can substitute for light to induce *ATH1* expression at the shoot apex. Furthermore, the relationship between sucrose and *ATH1* levels seems dose-dependent (Figs 1e, S2).

Importantly, these observations suggest a close correlation between *ATH1* transcript levels at the shoot apex and the extent to which rosette internode elongation is suppressed. We, therefore, analyzed elongation of vegetative internodes in dark-grown *35Spro: ATH1-HBD* plants exposed to increasing concentrations of Dex (Fig. 1f). Increased Dex-concentrations are expected to result in increased ATH1 levels in the nucleus and, hence, stronger inhibition of internode elongation. This was indeed observed, with a maximum inhibitory effect on internode elongation in plants exposed to 100 nM Dex (Fig. 1f). In line with this, dark-grown Col-8 plants displayed increasing inhibition of rosette internode elongation when exposed to increasing concentrations of sucrose, with complete restoration of internode compactness characteristic for rosette habit at 2.5% sucrose (Fig. 1f,g). As expected, in *ath1* mutants, internode elongation remained unaffected at all sucrose concentrations tested (Fig. 1g). This strongly suggests that sucrose-induced repression of rosette internode elongation in dark-grown plants is *ATH1*-dependent. These findings further show that loss of compact rosette habit, generally observed in sucrose-stimulated, dark-grown Arabidopsis plants, can be attributed to suboptimal *ATH1* expression at the shoot apex.

SAM morphology of sucrose-stimulated, dark-grown seedlings resembles that of light-grown *ath1* mutants

In light-grown *ath1* mutants, elongation of vegetative internodes results from premature RZ activity (Roldán *et al.*, 1999; Rutjens *et al.*, 2009; Ejaz *et al.*, 2021). To confirm that the elongated internode phenotype observed in dark-grown Arabidopsis plants also results from premature activation of stem development, we compared shoot apices of light- and dark-grown Col-8 seedlings with those of light-grown *ath1-4* seedlings (Fig. 2a–c). When grown for 5 d in continuous light, *ath1-4* mutants displayed elongated vegetative internodes, whereas those of Col-8 plants remained compact (Fig. S3a,c,f). Comparing both genotypes showed the four most apical cells of a central cell file running from the L1 layer into the subapical RZ region of the SAM to be of similar length. By contrast, more basal RZ cells were significantly more elongated in *ath1-4* mutants (Fig. 2a,c,f). A similar morphology was observed in dark-grown, sucrose-supplied Col-8 seedlings, where compact rosette habit is no longer maintained (Fig. S3b). Compared with light-grown seedlings, basal cells were significantly more elongated in dark-grown Col-8 seedlings, resembling the elongated RZ cells of light-grown *ath1-4* mutants. The four apical cells were of similar length in light- and dark-grown Col-8 seedlings (Fig. 2a–c,f).

Since ectopic expression of *ATH1* restored a compact rosette habit in dark-grown seedlings (Figs 1a,b, S3d–f), we examined whether this is caused by inhibition of RZ activity. Indeed, induction of *ATH1* specifically repressed cell elongation in the basal RZ cells (Fig. 2b,d–f). Taken together, these findings indicate that loss of rosette habit as a result of rosette internode elongation in the absence of light results from premature RZ activation due to significantly reduced *ATH1* expression at the shoot apex.

ATH1 functions downstream of multiple photoreceptors to maintain a compact rosette

Rosette internode elongation can also be observed in light-grown photoreceptor mutants, such as higher order phytochrome mutants and *phyB cry1* mutants (Devlin *et al.*, 1996, 1998, 1999, 2003; Whitelam & Devlin, 1997; Whitelam *et al.*, 1998; Roldán *et al.*, 1999; Mazzella *et al.*, 2000; Franklin *et al.*, 2003; Hu *et al.*, 2013). *ATH1* expression is strongly light-dependent (Fig. 1c,d), raising the question of whether light-mediated expression of *ATH1* depends on these photoreceptors. Analysis of *ATH1* mRNA levels in seedlings grown under different wavelengths of light revealed that apart from white light, monochromatic blue, red, and far-red light induce *ATH1* to significant levels, suggesting that *ATH1* is under control of multiple photoreceptors (Fig. 3a). We next determined *ATH1*-promoter activity and mRNA levels in a series of phytochrome and/or cryptochrome photoreceptor mutants grown under various light quality conditions (Figs 3c, S4a–d). In white light, *ATH1* levels were somewhat decreased in *phyB* and *cry1* single mutants, whereas combination of both mutations significantly affected *ATH1* expression (Figs 3c, S4a). Similarly, introduction of additional *phy* mutations in a *phyB* background or combination of the phytochrome chromophore biosynthesis mutant *hy1* with *cry1* and/or *cry2* mutations resulted in moderate to severe reduction in *ATH1* levels in white light, confirming that light-mediated *ATH1* expression is controlled by multiple photoreceptors (Figs 3c, S4a). Repeating experiments under monochromatic light conditions revealed that red-light-mediated induction of *ATH1* is mostly the result of phyB function, in cooperation with phyD and phyE, whereas phyA is largely responsible for *ATH1* induction in far-red light (Figs 3c, S4b,d). Under blue light, CRY1 and CRY2 redundantly contribute to *ATH1* activity, with CRY1 being the predominant cryptochrome under the conditions tested (Figs 3c, S4c). Moreover, all photoreceptor mutants previously reported to display loss of rosette habit due to elongation of vegetative internodes, including *phyBDE* and *phyB cry1* (Devlin *et al.*, 1998; Mazzella *et al.*, 2000), had severely reduced *ATH1* levels (Figs 3c, S4a–d).

Internode elongation reflects activity of the basal part of the SAM and is controlled by ATH1. Therefore, we compared the spatial activity of the *ATH1* promoter in *phyBDE* and *phyB cry1*

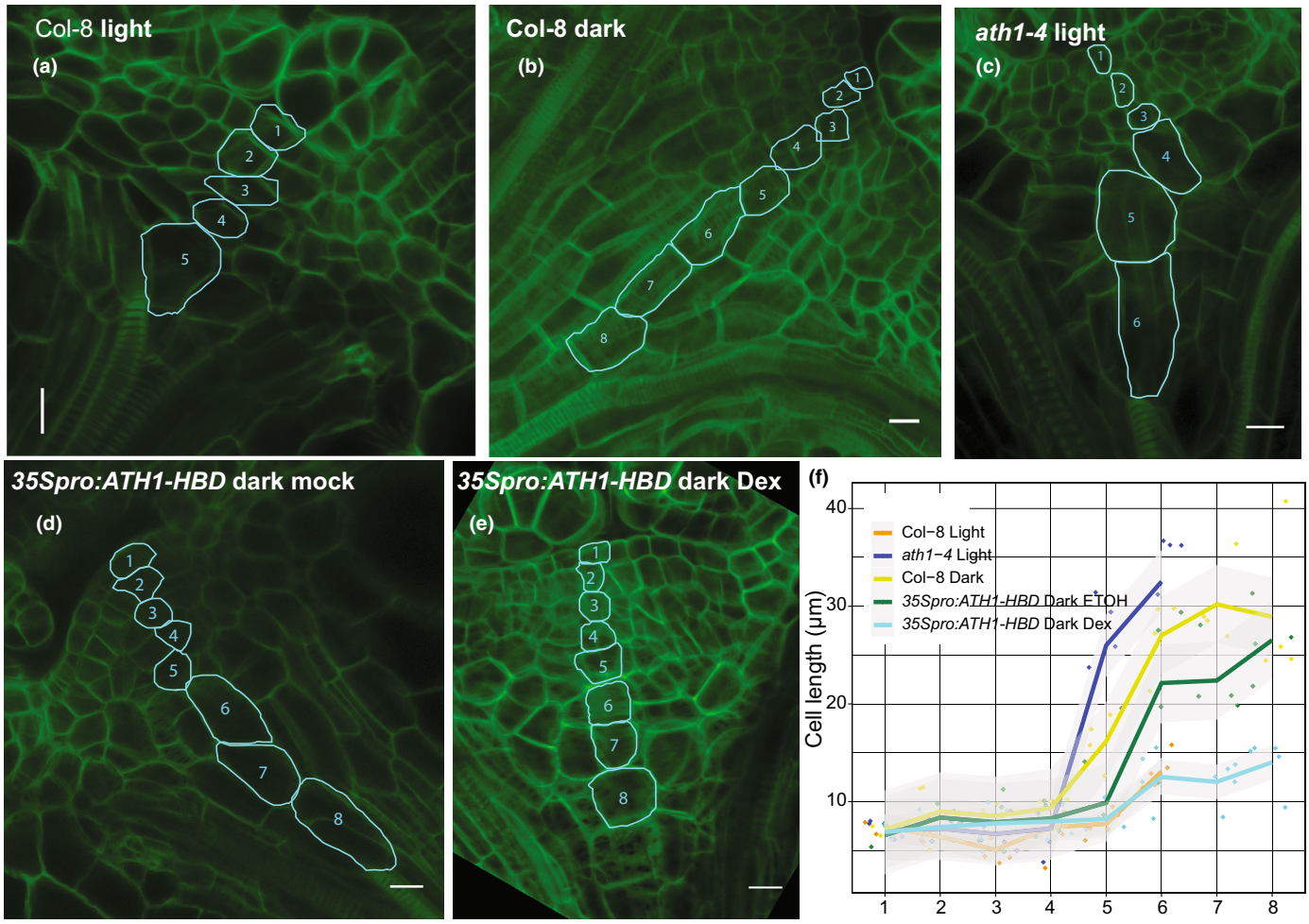

Fig. 2 Sugar-induced dark-grown *Arabidopsis thaliana* seedlings display a shoot apical meristem (SAM) morphology similar to light-grown *ath1* mutants. Median longitudinal optical sections through the shoot apical meristems of (a, b) 5-d-old Col-8, (c) *ath1-4*, and (d, e) *35Spro:ATH1-HBD* seedlings grown at 27°C in the presence (a, c) or absence (b, d, e) of light. Mock treatment (d) is 0.1% ethanol, Dex treatment (e) is 10 µM dexamethasone. Cells marked in cyan form a central cell file extending from the epidermis into the subapical region that forms the rib zone. Bars, 10 µm. (f) Quantification of cell lengths as illustrated in (a–e). The shaded areas around the lines represent the 95% confidence intervals. Individual cell lengths were measured per position in apical-basal direction. Per genotype and condition four or five individual apices were analyzed. The numbers on the *x*-axis correspond to the cell position as depicted in (a–e).

with that in L*er* control plants and a *phyB* mutant. High levels of GUS activity were present in the SAM and emerging leaf primordia of L*er* $ATH1_{pro}$:*GUS* seedlings grown in white light. Corroborating our qPCR data, GUS activity was significantly reduced in *phyB cry1* $ATH1_{pro}$:*GUS* and *phyBDE* $ATH1_{pro}$:*GUS* plants, whereas in a *phyB* background, GUS activity was only moderately affected (Fig. 3b). The most prominent effect of reduced photoreceptor signaling on *ATH1*-promoter activity was in the SAM. In both *phyB cry1* and *phyBDE*, GUS activity could hardly be detected in the SAM, including the RZ, whereas in leaf

Fig. 3 Significant reduction in *ARABIDOPSIS THALIANA HOMEOBOX GENE1* (*ATH1*) expression levels underlies loss of compact rosette habit in *Arabidopsis thaliana* photoreceptor mutants. (a) Expression of *ATH1* in 7-d-old seedlings (L*er*) grown in SD white light (WL), red (RL), blue (BL), far-red light (FRL) or continuous darkness (DRK). Transcript levels were normalized to *GAPC2* (AT1G13440). Dots indicate the average values of four biological replicates per light treatment, each consisting of 40–50 seedlings. (b) Shoot apices of β-glucuronidase (GUS)-stained, 7-d-old $ATH1_{pro}$:*GUS* seedlings in different genetic backgrounds (Col-8, *phyB*, *phyBcry1*, and *phyBDE*). Plants were grown in white light under short-day conditions. Scale bars represent 0.01 mm. (c) Heat map generated from qPCR data on relative *ATH1* expression in indicated photoreceptor mutants (see Supporting Information Fig. S1), when compared to wild-type (WT) control plants (L*er* and Col-8). Transcript levels were normalized to *GAPC2* (AT1G13440; BL) or *MUSE3* (AT5G15400; RL, FRL and WL). The average of three biological replicates is shown, each replicate consisting of 40–50 seedlings. Red corresponds to high relative expression and dark blue corresponds to low relative expression. A linear fold change scale is displayed on top. (d) Average rosette internode elongation in WT (L*er*), *phyB*, *phyBcry1*, *hy1cry1*, and *hy1cry1cry2* in the absence or presence of a Pro_{35S}:*HA-ATH1* transgene. Plants were grown under long day (LD) conditions. In (a, d) different letters denote statistically significant differences between groups ($P < 0.05$) as determined by a one-way analysis of variance with Tukey's honest significant difference *post hoc* test (a) or a multiple comparison analysis using the Dunn Test with the Benjamini–Hochberg method (d). Colored dots indicate the average rosette internode length per individual ($n \geq 16$ individual plants per genotype). (e) Representative plants from (d). Arrows indicate elongated rosette internodes; arrowheads indicate complete suppression of internode elongation. Bars, 5 mm. In boxplot (a) and violin plot (d), the center bar indicates median values, box edges correspond to interquartile ranges (IQR), and error bars display values within 1.5 × IQR, with circular points as outliers. Violin plot width represents data density at specific values.

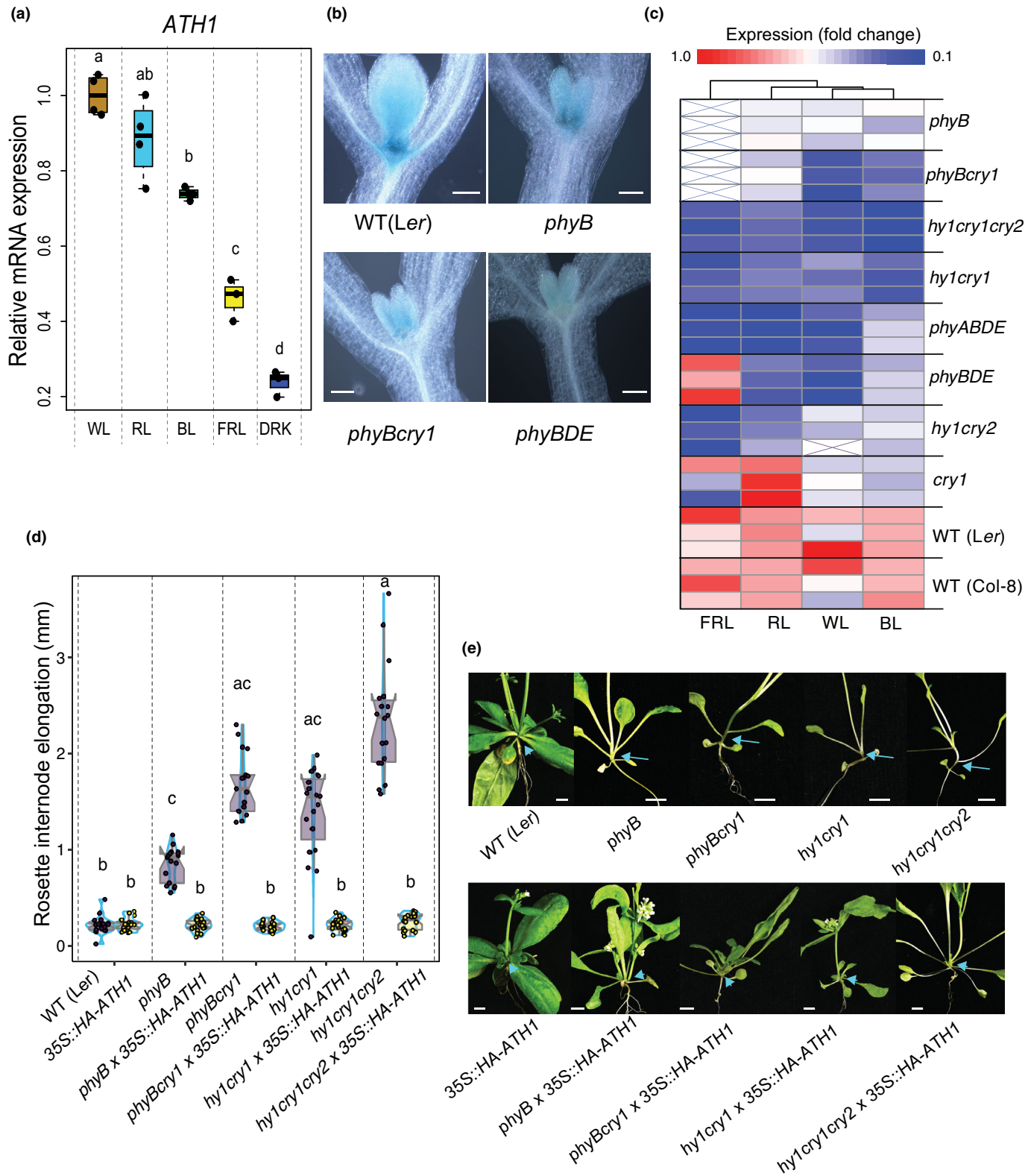

primordia, a more modest reduction was observed (Fig. 3b). Taken together, these findings suggest that phytochrome and cryptochrome photoreceptor families contribute to compact rosette habit in Arabidopsis through induction of *ATH1* expression in the SAM.

This was further tested by constitutively expressing *ATH1* in a number of photoreceptor mutants that display elongation of vegetative internodes when grown under standard, long-day conditions. Under these conditions, L*er* control plants never display detectable elongation of rosette internodes. By contrast,

internodes of *phyB*, *phyBcry1*, *hy1cry1*, and *hy1cry1cry2* mutants were visibly elongated, and the extent to which rosette internode elongation was affected correlated with *ATH1* levels in respective mutants (Figs 3c–e, S4a). As expected, constitutive expression of *ATH1* completely suppressed internode elongation in these mutants (Fig. 3d,e). Thus, establishing high levels of *ATH1* is sufficient to restore internode compactness of rosette habit in higher order photoreceptor mutants.

In conclusion, compact rosette habit, quintessential for light-grown Arabidopsis plants, is imposed by *ATH1* activity in the shoot apex under control of multiple blue and red/far-red light photoreceptors.

Light-mediated *ATH1* expression is controlled by central light-signaling components

ATH1 was first identified as a light-regulated gene that is derepressed in dark-grown *cop1* mutants (Quaedvlieg *et al.*, 1995). COP1, in conjunction with SPA proteins, functions as a repressor of light signaling in darkness. In light, activated phytochrome and cryptochrome family members suppress the activity of the COP1/SPA complex to promote photomorphogenesis (Ponnu & Hoecker, 2021). Light-mediated *ATH1* expression involves both phytochrome and cryptochrome family members. Since COP1 is a downstream signaling component of these photoreceptor families, we analyzed the role of COP1 in the regulation of *ATH1* expression and compactness of vegetative internodes. First, we compared *ATH1* expression levels between dark-grown Col-8 and *cop1-4* seedlings, with and without added sucrose (Fig. 4a). In line with Quaedvlieg *et al.* (1995), in dark-grown *cop1-4* mutants, carrying a mild loss-of-function allele of *COP1*, *ATH1* expression was clearly derepressed. Already in the absence of sucrose, *ATH1* accumulated to higher levels than observed in sucrose-supplied Col-8 plants. In the presence of sucrose, *cop1-4 ATH1* transcript levels increased even further (Fig. 4a), indicating that light and sucrose signaling contribute, at least partially, independently to induce *ATH1* expression.

Accordingly, vegetative internodes of sucrose-supplied, dark-grown *cop1-4* mutants did not elongate, contrasting to those of Col-8 plants (Fig. 4b,c). A compact growth habit in darkness is lost in *cop1-4 ath1-4* double mutants, indicating that this phenotype requires ATH1 (Fig. 4c). However, compared with *ath1-4*, internode elongation in *cop1 ath1* double mutants is still much reduced, suggesting the involvement of other loci apart from *ATH1* (Fig. 4b,c).

Like COP1, PIFs also function as downstream components in both phytochrome and cryptochrome light signaling (Ma *et al.*, 2016; Pedmale *et al.*, 2016; Pham *et al.*, 2018b). PIF proteins function as partially redundant, negative regulators of light responses to maintain skotomorphogenesis in dark-grown seedlings. Upon exposure to light, phytochromes promote the turnover of PIFs, whereas photoactivated CRY1 interacts with PIF4, resulting in suppression of PIF4 transcriptional activity (Ma *et al.*, 2016). As a consequence, plants switch from

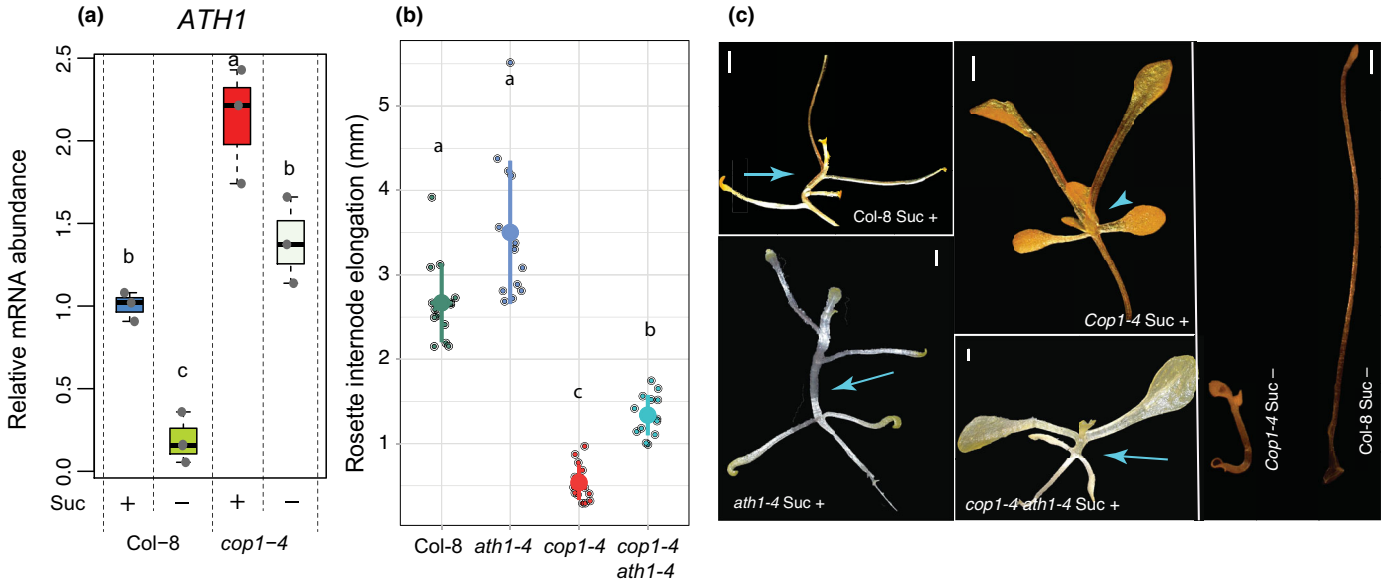

Fig. 4 Derepression of *ARABIDOPSIS THALIANA HOMEOBOX GENE1* (*ATH1*) contributes to a compact rosette habit in dark-grown *cop1* mutants. (a) Relative mRNA abundance of *ATH1* in shoot apices of 2-wk-old dark-grown *Arabidopsis thaliana* seedlings. The average of three biological replicates is shown. At least 20 shoot apices were used for each biological replicate. (b) Average rosette internode lengths of 3-wk-old Col-8, *ath1-4*, *cop1-4*, and *cop-1 ath1-4* plants ($n \geq 13$) grown in continuous darkness for 3 wk at 22°C, in the presence of 1% sucrose. In (a, b) different letters denote statistically significant differences between groups ($P < 0.05$) as determined by a one-way analysis of variance with Tukey's honest significant difference *post hoc* test for (a) and a multiple comparison analysis using the Dunn Test with the Benjamini–Hochberg method for (b). (c) Representative plants from (b). Arrows indicate elongated rosette internodes, arrowheads indicate complete suppression of internode elongation. Bars, 0.5 mm. Sucrose (Suc +) or sorbitol (Suc −), both to a final concentration of 1%, were added 3 d after start of the experiment (a, c). In boxplot (a), the center bar indicates median values, box edges correspond to interquartile ranges (IQR), and error bars display values within 1.5× IQR, with circular points as outliers. In dotplot (b), colored dots represent individual data points and overlaid summary statistics display mean values as larger dots and error bars for one standard deviation.

skotomorphogenesis to photomorphogenesis. In line with this, quadruple *pif1pif3pif4pif5* (*pifq*) mutants display a constitutively photomorphogenic phenotype in darkness (Leivar *et al.*, 2009). In addition, PIFs can directly interact with COP1, thereby enhancing substrate recognition and ubiquitination activity of the COP1 E3 ligase complex (Xu *et al.*, 2014; Kathare *et al.*, 2020). Therefore, we tested whether PIF proteins might function upstream of *ATH1* in the regulation of compact rosette habit. To this end, we analyzed rosette internode compactness in a series of sucrose-supplied, dark-grown single, double, triple, and quadruple *pif* mutant combinations. In *pifq* mutants, complete repression of rosette internode elongation was observed, resulting in the formation of a compact rosette in darkness (Fig. 5a). None of the double or triple mutants tested were as compact as the quadruple *pifq* mutant, whereas of the single mutants tested, only *pif4* displayed a significant reduction in rosette internode length when compared to control plants (Fig. 5a). This indicates that PIF1, PIF3, PIF4, and PIF5 redundantly contribute to rosette internode elongation in etiolated plants. Of these, PIF4 contributes the most, as can be inferred from its mutant phenotype and the significant inhibition of internode elongation in higher order mutants carrying a *pif4* allele, while inhibition of internode elongation is absent in *pif1pif3* and only subtly enhanced by *pif5* mutation in *pif4pif5* and *pif3pif4-pif5* (Fig. 5a).

Next, we compared *ATH1* transcript levels between shoot apices of dark-grown Col-8, *pif4* and *pifq* plants (Fig. 5b). In line with the observed rosette internode lengths, a significant increase in *ATH1* was seen in both *pif4* (1.7×) and *pifq* (3×) mutants when compared to control plants. To examine whether ATH1 is responsible for the inhibition of rosette internode elongation in dark-grown *pifq* mutants, we combined *ath1-3* and *pifq* mutations. Surprisingly, vegetative internodes of sucrose-supplied, dark-grown *pifq ath1* plants were only mildly elongated, resulting in partial loss of a compact rosette habit. Compared to *ath1* plants, *pifq ath1* internodes were on average 70% shorter (Fig. 5c). This might suggest that PIFs control rosette internode elongation mostly independent of ATH1. Alternatively, the relationship between PIFs and ATH1 could be more complex. ATH1-PIF feedback regulation would explain for the *pifq ath1* internode phenotype. Recently, *PIF4* was identified as binding target of ATH1, but no significant differences in *PIF4* expression could be detected between *ath1* and WT plants on whole-seedling basis (Ejaz *et al.*, 2021). This does not rule out a tissue-specific, regulatory feedback loop between ATH1 and PIFs. To explore the presence of such regulatory interaction between ATH1 and PIFs, we quantified *PIF* transcript levels in shoot apices of genotypes with altered *ATH1* expression (Fig. 5d,e). ATH1 is expected to have an inhibitory effect on *PIF* expression and in sucrose-supplied, dark-grown plants *ATH1* levels are low (Fig. 1c,d). Therefore, *35Spro:ATH1-HBD* plants were used to examine the effect of ATH1 on *PIF1*, *PIF3*, *PIF4*, and *PIF5* mRNA levels in dark conditions (Fig. 5d). In light-grown vegetative plants, *ATH1* levels at the shoot apex are relatively high. Therefore, in light conditions, the effect of ATH1 on these *PIFs* was analyzed using *ath1-3* plants (Fig. 5e). In both conditions, a clear effect of ATH1 on *PIF* expression was observed. In dark-grown plants, induction of ATH1 resulted in significant downregulation of *PIF1*, *PIF3* and *PIF4*, and, to a lesser extent, *PIF5* (Fig. 5d). In light-grown plants, *PIF1*, *PIF3*, *PIF4*, and *PIF5* levels were significantly upregulated in the absence of *ATH1* (Fig. 5e). Thus, ATH1 acts as a negative regulator of *PIF1*, *PIF3*, *PIF4*, and *PIF5* in the shoot apex. Together, our data support the presence of a double-negative transcriptional feedback loop between ATH1 and PIF family members. Such ATH1-PIF interdependence for suppression of rosette internode elongation explains the observed incomplete loss of rosette habit compactness in *cop1-4 ath1-4* mutants (Fig. 4b,c), since PIF1, PIF3, PIF4, and PIF5 are required for dark-mediated rosette internode elongation in the absence of ATH1 (Fig. 5c) and these PIFs are degraded in darkness in the presence of a *cop1-4* mutation (Pham *et al.*, 2018a,c).

Overall, our data show that loss of internode compactness and thereby loss of rosette habit in dark-grown Arabidopsis plants is part of a skotomorphogenesis program, achieved through active repression of *ATH1*, mediated by COP1 and PIF proteins.

Photosynthesis-derived sugars are no prerequisite for light-induced *ATH1* expression

ATH1 expression in the shoot apex can be induced by light and sucrose (Figs 1d,e, 3a). Since light acts as both a developmental signal, and an energy source through photosynthesis, we investigated the exact role of light in induction of *ATH1* expression. Therefore, we examined *ATH1*-promoter activity in plants where photosynthesis was inhibited. To this end, $ATH1_{pro}$*:GUS* seedlings were grown in darkness for 5 d, without sucrose to deplete plant metabolizable sugar. Five hours before light treatment, plants were put in a CO_2-deficient environment, after which plants were grown for 2 d in continuous light (Fig. 6a). CO_2 removal inhibits photosynthetic carbon assimilation and, thereby, accumulation of sugars. Compared with mock treatment, *ATH1*-promoter activity was decreased, but GUS staining was still clearly visible (Figs 6b, S5a). Similarly, chemical inhibition of photosynthesis by adding norflurazon or lincomycin resulted in slightly reduced *ATH1* expression (Figs S5a, S6). This indicates that *ATH1* is affected by light acting as both a developmental trigger and an energy source through photosynthesis. It further shows that photosynthesis-derived sucrose contributes to, but is not a prerequisite for light-induced *ATH1* expression. This is in line with the observation that *ATH1* is derepressed in dark-grown *cop1* seedlings even in the absence of sucrose (Fig. 4a).

Sugars function as energy resource and as signaling molecules (Li & Sheen, 2016). To distinguish between these functions in the induction of *ATH1*, *ATH1* expression and *ATH1*-promoter activity were determined in dark-grown Col-8 plants supplied with either sorbitol, sucrose, glucose, fructose, or palatinose (Figs 6c, S5c). Glucose, fructose, and sucrose are metabolizable sugars also known to function as signaling molecules (Rabot *et al.*, 2012). Sorbitol and palatinose are nonmetabolizable sugars, but where palatinose can function as signaling molecule, sorbitol is neither metabolized nor signaling molecule (Ramon

et al., 2008). Neither sorbitol nor palatinose had a significant effect on *ATH1* expression, whereas a clear increase in *ATH1* could be observed when either sucrose, glucose, or fructose was present (Fig. 6c). This strongly suggests that sugars as energy source induce *ATH1* expression.

Sucrose and light independently regulate *ATH1* expression via TOR kinase

TOR kinase, a critical sensor of resource availability, is required for the activation of shoot and root apical meristems (Xiong

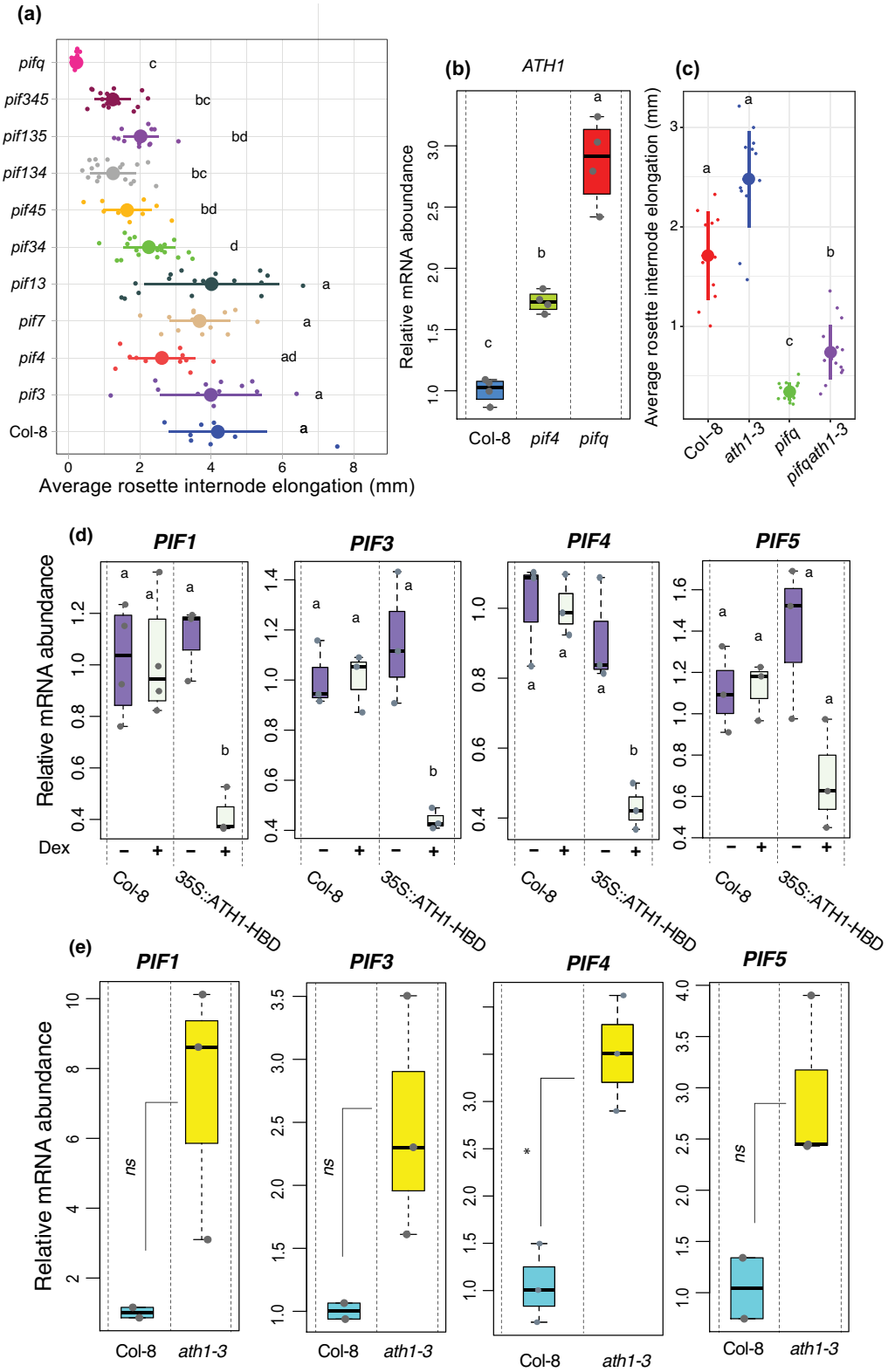

Fig. 5 A double-negative feedback loop between *ARABIDOPSIS THALIANA HOMEOBOX GENE1* (*ATH1*) and PHYTOCHROME INTERACTING FACTORS (PIFs) is required for initiation and maintenance of rosette growth habit *in Arabidopsis thaliana*. (a) Average internode lengths of 3-wk-old Col-8, *pif3*, *pif4*, *pif7*, *pif1pif3*, *pif3pif4*, *pif4pif5*, *pif1pif3pif4*, *pif1pif3pif5*, *pif3pif4pif5*, and *pifq* (*pif1pif3pif4pif5*) plants grown in continuous darkness at 22°C. Sucrose was added to the medium to a final concentration of 1% 3 d after the start of the experiment. Colored dots indicate average rosette internode elongation scores of individual seedlings ($n \geq 9$). (b) Relative mRNA abundance of *ATH1* in shoot apical meristem (SAM)-enriched tissue of 14-d-old, dark-grown Col-8, *pif4*, and *pifq* seedlings ($n \geq 20$ per biological replicate; four biological replicates). Transcript levels were normalized to *GAPC2* (AT1G13440). Sucrose was present at a 1% final concentration from the start of the experiment. (c) Average internode lengths of 3-wk-old Col-8, *pif4*, *pifq*, and *pifq ath1-3* plants grown in continuous darkness at 22°C. Sucrose was added to the medium to a final concentration of 1% 3 d after the start of the experiment. Colored dots indicate average rosette internode elongation scores of individual seedlings ($n \geq 11$). (d, e) Relative mRNA abundance of indicated *PIF* genes in SAM-enriched tissue of 14-d-old, dark-grown Col-8 and *35Spro:ATH1-HBD* ($n \geq 3$) (d), or 39-d-old, light-grown (SD conditions) Col-8 and *ath1-3* seedlings ($n \geq 2$) (e). For (d) seedlings were treated with a mock (0.1% ethanol, Dex −) or 10 μM dexamethasone (Dex +) at day three, and in total, 30–40 shoot apices were used for each biological replicate. For light-grown plants (e), three shoot apices were used per biological replicate. Transcript levels were normalized to *GAPC2* (AT1G13440). Seedlings were treated with a mock (0.1% ethanol, Dex −) or 10 μM dexamethasone (Dex +) (d). In (a–d) different letters denote statistically significant differences between groups ($P < 0.05$) as determined by a one-way analysis of variance with Tukey's honest significant difference *post hoc* test for (b, d) and a multiple comparison analysis using the Dunn Test with the Benjamini–Hochberg method for (a, c). In (c), the Kruskal–Wallis test utilized to distinguish significant differences between groups, with results of *P*-values depicted as 'ns' for nonsignificant and an asterisk (*) for a *P*-value of 0.04953. In dotplots (a, c), colored dots represent individual data points and overlaid summary statistics display mean values as larger dots and error bars for one standard deviation. In boxplots (b, d, e), the center bar indicates median values, box edges correspond to interquartile ranges (IQR), and error bars display values within 1.5× IQR, with circular points as outliers.

et al., 2013; Pfeiffer *et al.*, 2016; Li *et al.*, 2017). It integrates, among others, energy and environmental cues, including light signals to direct growth and development. The fundamental role of TOR kinase downstream of light and energy signals led us to investigate whether TOR activity is needed for sugar-dependent, dark morphogenesis in general and *ATH1* induction in particular. Employing a similar experimental setup as mentioned in the previous section (Fig. 6a), the effect of the TOR kinase inhibitor AZD-8055 (Montané & Menand, 2013; Dong *et al.*, 2015) on light- and sucrose-induced *ATH1*-promoter activity was studied. Light-mediated induction was efficiently suppressed by AZD-8055, resulting in complete inhibition of promoter activity at a concentration 0.5 μM (Fig. 6d). Similarly, AZD-8055 fully inhibited the positive effect of sucrose on *ATH1* (Figs 6e, S5b, S7). In line with these findings, conditional silencing of *AtTOR* in *35S:ALCR alcA:RNAi-TOR* seedlings (Deprost *et al.*, 2007) led to complete inhibition of sucrose-mediated induction of *ATH1* (Fig. 6f). When applied for an extended period, in the presence of sucrose, AZD-8055 inhibited dark-morphogenesis in a dose-dependent manner (Fig. S8a,b), indicating that, next to *ATH1* induction, TOR activity is necessary for sucrose-dependent, dark morphogenesis in general.

TOR kinase has been reported to contribute to seedling de-etiolation and COP1 represses TOR activity during skotomorphogenesis (Chen *et al.*, 2018). We therefore tested whether COP1-mediated regulation of *ATH1* is TOR-dependent. This is indeed the case, as in the presence of AZD-8055 *ATH1* is no longer derepressed in dark-grown *cop1-4* plants (Fig. S9).

TOR kinase, thus, integrates light and sucrose signals leading to activation of *ATH1* gene expression at the shoot apex. Upstream of TOR kinase, a PHY-COP1 regulatory pathway functions as negative regulator of TOR activity. In darkness, COP1 inhibits TOR, resulting in repression of *ATH1*. As a consequence, in dark-grown plants, a compact rosette habit is lost due to activation of stem development. In light, COP1 activity is inhibited allowing for TOR kinase to induce *ATH1* as part of the de-etiolation process, resulting in a compact rosette characteristic for *A. thaliana* (Fig. 7). TOR was recently reported to control cytokinin homeostasis at the SAM by translational repression of several mRNAs encoding cytokinin catabolic enzymes, including the RZ-expressed CYTOKININ OXIDASE/DEHYDROGENASE5 (CKX5) (Janocha *et al.*, 2021). Adding cytokinin to dark-grown Arabidopsis seedlings results in strong induction of *ATH1*-promoter activity, even in the absence of metabolizable sugar (Fig. S10), suggesting that TOR-mediated regulation of *ATH1* might be indirect through cytokinin.

Discussion

In plants, most of the adult body is formed postembryonically by the continuous activity of the shoot and root apical meristems. At the completion of embryogenesis, these meristems are quiescent, but become reactivated after germination. In Arabidopsis, light is crucial for SAM reactivation (López-Juez *et al.*, 2008; Pfeiffer *et al.*, 2016; Mohammed *et al.*, 2017). A direct outcome of this is the production of leaves. In rosette plants, such as Arabidopsis, these leaves give rise to a basal rosette: a whorl of leaves without elongation between successive nodes. The rosette habit is widespread amongst flowering plants and provides several advantages compared to taller, less compact plants, such as protection from (a)biotic stresses (Schaffer & Schaffer, 1979; Bello *et al.*, 2005; Larcher *et al.*, 2010; Thomson *et al.*, 2011; Fujita & Koda, 2015). In Arabidopsis, light requirement for SAM activation can be overcome by availability of metabolizable sugars to the meristem (Araki & Komeda, 1993; Roldán *et al.*, 1999). However, under such conditions, plants fail to establish a compact rosette. Instead, they display a caulescent growth habit due to elongation of rosette internodes. Here, we show that this dramatic change in growth habit in the absence of light is caused by premature RZ activation due to insufficient expression of the light-induced *ATH1* gene at the SAM. Our observations confirm a fundamental role for ATH1 in Arabidopsis rosette habit and support a role for TOR kinase as central hub for integration of energy and light signaling in controlling cell differentiation and organ initiation at the SAM.

Previously, activation of the SAM following germination, via induction of *WUSCHEL* (*WUS*), and subsequent initiation of leaf primordia were shown to be synergistically controlled by

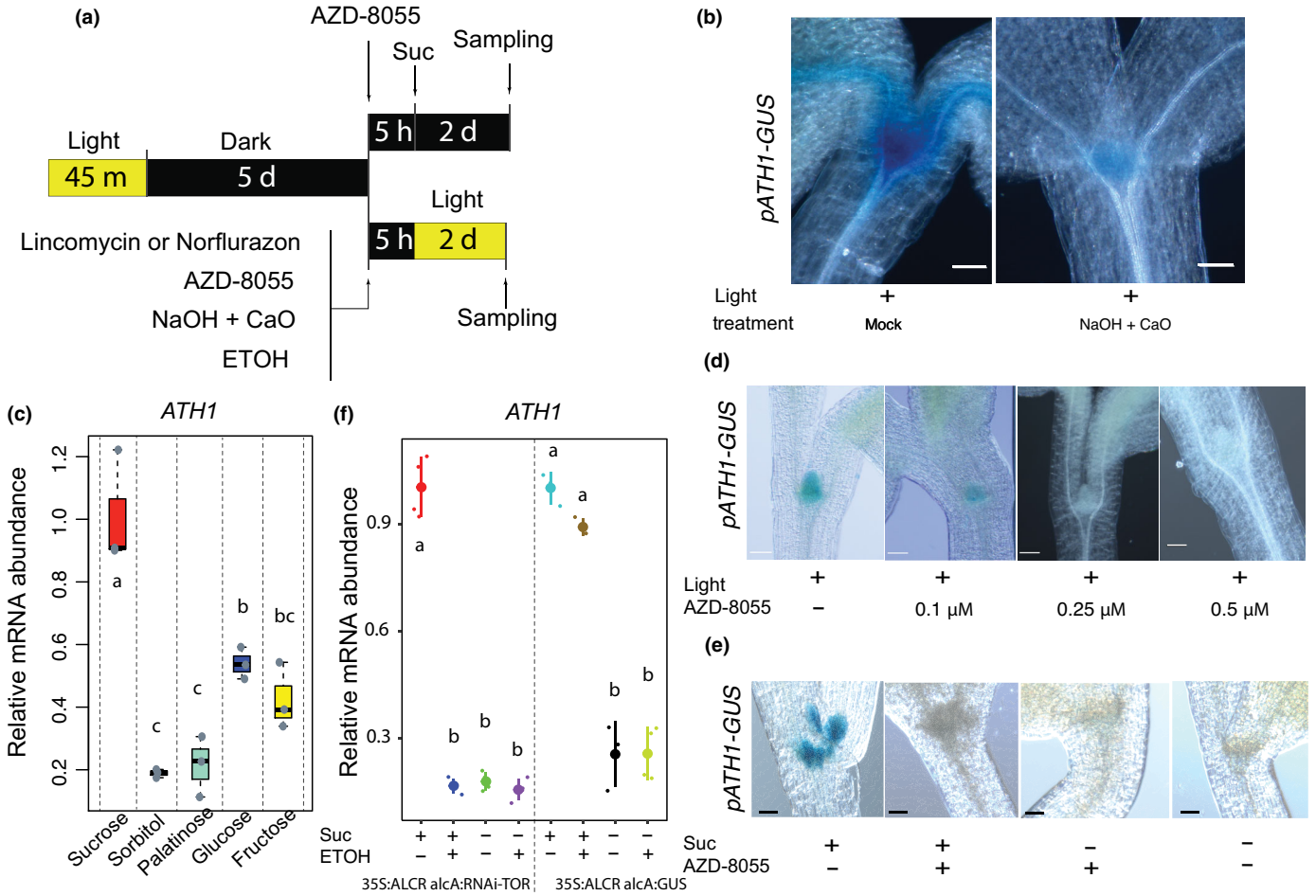

Fig. 6 *ARABIDOPSIS THALIANA HOMEOBOX GENE1* (*ATH1*) expression is independently regulated by light and sucrose. (a) Schematic representation of the experimental setup. *Arabidopsis thaliana ATH1$_{pro}$:GUS* seeds were light-treated for 45 min to stimulate germination, before growth in continuous darkness for 5 d. AZD-8055, lincomycin, norflurazon were then added or CO_2 was removed (NaOH + CaO) and seedings were grown for an additional 5 h in darkness before switching to *ATH1*-inducing conditions (continuous light or continued growth in darkness in the presence of sucrose (Suc)) for two more days. (b) Shoot apices of β-glucuronidase (GUS)-stained *ATH1$_{pro}$:GUS* seedlings grown in CO_2-free air (NaOH + CaO), according to the scheme depicted in (a). Mock-treatment was without NaOH + CaO. Bars, 0.05 mm. (c) Relative expression of *ATH1* in 7-d-old, dark-grown seedlings, grown in the presence of either sucrose, glucose, fructose, palatinose, or sorbitol, all at a final concentration of 1% in the growth medium. Sugars were added at the start of the experiment. Transcript levels were normalized to *MUSE3* (At5g15400). The average of three biological replicates is shown. At least 30 seedlings were used for each biological replicate. (d, e) Shoot apices of GUS-stained *ATH1$_{pro}$:GUS* seedlings treated with the Target of Rapamycin (TOR) kinase inhibitor AZD-8055 before switching to ATH1-inducing conditions (continuous light (d) or darkness in the presence of 1% sucrose (e)) according to the scheme depicted in (a). Bars, 0.01 mm. (f) Relative expression of *ATH1* in 7-d-old, dark-grown *35S::ALCR alcA : RNAi-TOR* and *35S:ALCR alcA:GUS* (control line) seedlings in the presence or absence of ethanol (ETOH; 0.1%) and/or sucrose (Suc; 1%), as depicted in (a). ETOH was added after 5 d of growth in darkness. After an additional 5 h in darkness sucrose was added and plants were sampled after two more days in darkness. Transcript levels were normalized to *GAPC2* (AT1G13440). The average of three biological replicates is shown. At least 30 seedlings were used for each biological replicate. In (c, f) different letters denote statistically significant differences between groups ($P < 0.05$) as determined by one-way ANOVA followed by Tukey's *post hoc* test. In boxplot (c), the center bar indicates median values, box edges correspond to interquartile ranges (IQR), and error bars display values within 1.5× IQR, with circular points as outliers. In dotplot (f), colored dots represent individual data points and overlaid summary statistics display mean values as larger dots and error bars for one standard deviation.

light-signaling pathways and photosynthesis-derived sugars, both conveyed by TOR kinase (Pfeiffer *et al.*, 2016; Li *et al.*, 2017). In line with this, we show that TOR activity is necessary for sugar-induced, dark morphogenesis in Arabidopsis. Furthermore, we show that *ATH1* expression at the SAM, required to inhibit RZ activation during vegetative development, is additively induced by sugar and light-signaling and that TOR kinase activity is essential for both. Thus, TOR kinase not only integrates light and energy signals to activate the central stem cell population and subsequent differentiation processes at the meristem periphery, but also to repress differentiation processes at the basal part of the meristem by inhibiting RZ activity. Potentially, induction of *ATH1* through light and energy signals might result from SAM activation. This appears unlikely, as in the absence of sucrose the SAM of dark-grown *cop1* mutants remains dormant, while *ATH1* is expressed to relatively high levels. In addition, SAM activation and *ATH1* induction responses differ in their sensitivity to sucrose. Concentrations adequate to activate the SAM and initiate organogenesis, fail to induce significant levels of *ATH1*.

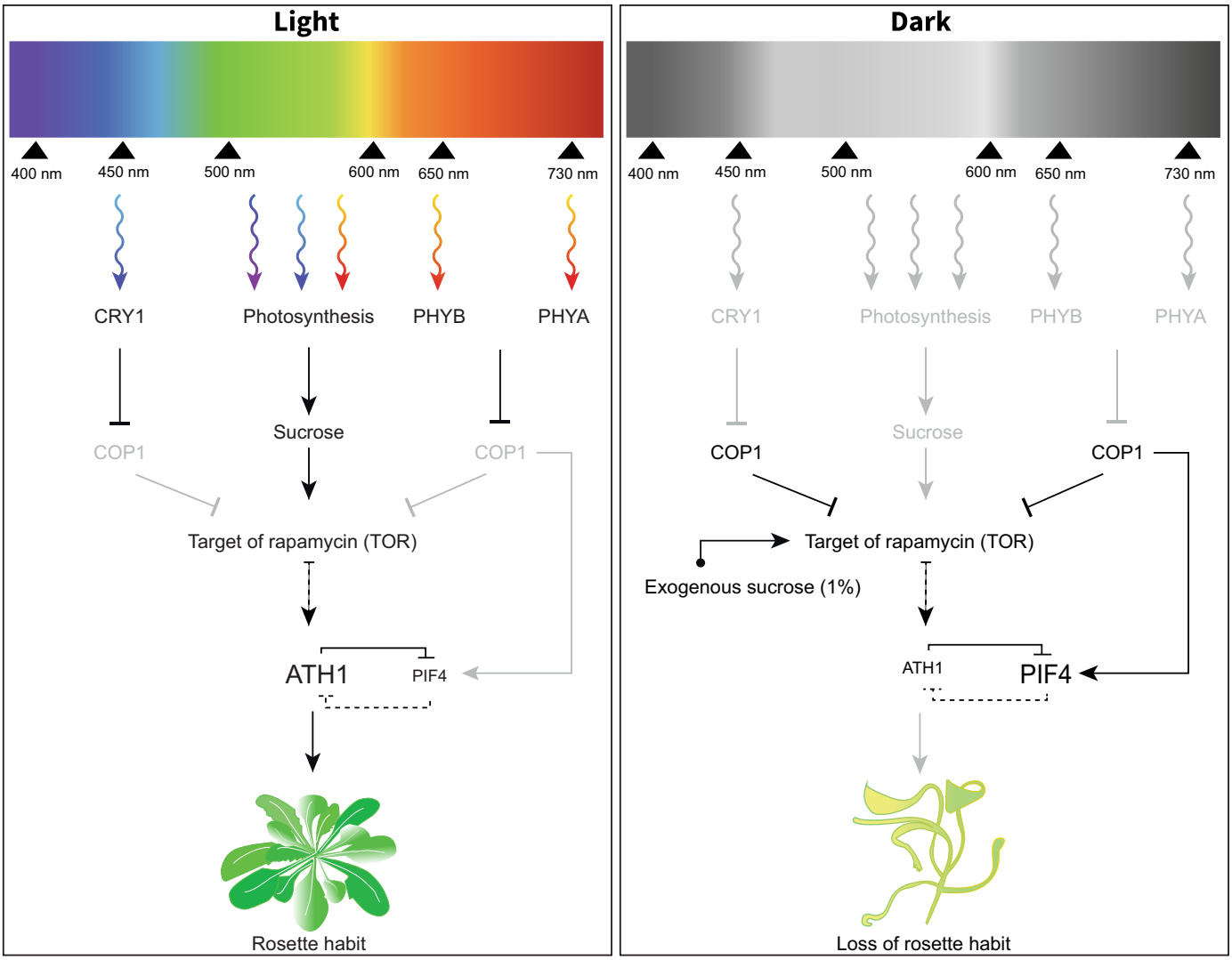

Fig. 7 Light and sucrose signaling pathways converge at Target of Rapamycin (TOR) kinase to control *ARABIDOPSIS THALIANA HOMEOBOX GENE1* (*ATH1*) expression and subsequent rosette growth habit in *Arabidopsis thaliana*. (left panel) Expression of *ATH1* is mediated by the activity of TOR kinase in response to both sugar and light. In response to light, photoreceptor signaling inhibits the activity of a CONSTITUTIVE PHOTOMORPHOGENIC1 (COP1)-containing protein complex that acts as a central repressor of light signaling in darkness. This releases the inhibitory effect of COP1 on TOR kinase. Activation of TOR kinase then leads to both activation of the shoot apical meristem (SAM) and induction of *ATH1* expression in the SAM. As a consequence of *ATH1* expression in the SAM, *PIF* gene expression, including *PIF4*, is locally inhibited. This contributes to inhibition of rib zone activity and, consequently, suppression of rosette internode elongation with the for Arabidopsis typical rosette growth habit as a result. As TOR kinase is a major regulator of mRNA translation, the effect on *ATH1* expression is most likely indirect (dotted arrow). (right panel) In the absence of light, the COP1-complex is stabilized and inhibits TOR kinase activity and subsequent SAM activation. In addition, the COP1-complex stabilizes PHYTOCHROME INTERACTING FACTOR (PIF) proteins in darkness to positively regulate skotomorphogenesis. As a combined effect, *ATH1* is not expressed under these conditions. As discussed, the PIF inhibitory effect on *ATH1* expression, including that of PIF4, is most likely indirect (dotted inhibitory arrow). Sucrose-availability to the SAM can substitute for light both in the case of SAM activation and for *ATH1* induction. Although both processes are mediated through TOR kinase, sucrose levels sufficient to activate the SAM only result in weak expression of *ATH1*, probably as the result of still active COP1-PIF signaling. Resulting ATH1 levels are insufficient to suppress rib zone activity. As a consequence, in most circumstances sugar-induced dark-grown seedlings display a caulescent growth habit due to premature rib zone activation resulting in elongation of vegetative internodes. Blunt-ended arrows indicate an inhibitory effect. Arrows in grey indicate the absence of specified inhibitory or activation effects under the given conditions.

How TOR kinase controls *ATH1*-promoter activity is currently unknown. TOR is a major regulator of translation (Schepetilnikov & Ryabova, 2017). Active TOR promotes translation of mRNAs harboring uORFs within their leaders, by triggering reinitiation after uORF translation (Schepetilnikov *et al.*, 2011, 2013). *ATH1* carries a 1279-nt leader sequence, containing seven AUG-containing uORFs. However, for ATH1, we do not expect TOR-mediated translational control to be a major type of regulation. First, none of the seven *ATH1* uORFs seems to be translated (Hu *et al.*, 2016). Second, a close correlation can be observed between *GUS* mRNA levels and GUS activity in our $ATH1_{pro}$:*GUS* line, a translational fusion that contains the entire *ATH1* leader sequence (compare Figs 1e and S8; S7). Together, this argues against strong uORF-mediated translational control of ATH1. Therefore, the effect of TOR kinase on *ATH1* is, most likely, indirect, possibly through TOR-mediated regulation of

cytokinin homeostasis, as was previously reported for *WUS* (Janocha *et al.*, 2021).

In the absence of light, *ATH1* is repressed by negative regulators of photomorphogenesis, including COP1, fitting with previous finding that in darkness COP1 represses TOR kinase (Chen *et al.*, 2018). Here, we report that, in darkness, sucrose can substitute for light to induce *ATH1* and this also requires TOR kinase (Fig. 7). Most likely, sucrose affects TOR kinase activity independently of COP1 since sucrose-mediated induction of *ATH1* can still be observed in a *cop1* background. Light signaling inactivates COP1, resulting in induction of auxin biosynthesis. Auxin then activates the small Rho-like GTPase ROP2, which in turn activates TOR (Cai *et al.*, 2017; Li *et al.*, 2017; Schepetilnikov *et al.*, 2017). Constitutive expression of activated ROP2 stimulates TOR in the shoot apex and is sufficient to promote organogenesis in the absence of light (Li *et al.*, 2017). Sugars are known to trigger the accumulation of auxin, along with its biosynthetic precursors and such sucrose-induced auxin might activate TOR kinase in darkness, in the presence of COP1 (Chourey *et al.*, 2010; LeClere *et al.*, 2010; Sairanen *et al.*, 2012; Mohammed *et al.*, 2017). Worth mentioning in this respect is that the same PIF proteins identified here as repressors of *ATH1*, repress sugar-induced auxin biosynthesis (Sairanen *et al.*, 2012).

Similar to the peripheral zone, where lateral organs are generated, the RZ, where differentiation into stem tissue occurs, is continuously replenished by a population of dividing stem cells in the central zone of the SAM. An active central stem cell population is therefore a prerequisite for RZ activity. When TOR kinase is inactive, quiescence of the shoot stem cell population (Fig. S8) prevents the RZ being activated, even though ATH1-mediated inhibition of RZ activity is absent (Fig. S7). In light-grown or sucrose-supplemented dark-grown Arabidopsis seedlings, activated TOR kinase allows for stem cell activation. However, subsequent activation of the RZ is prevented via TOR-kinase-mediated ATH1 induction. In the presence of light, *ATH1* expression is induced in a functionally redundant manner by multiple photoreceptors operating in response to broad wavelengths of light (Fig. 7). This ensures the presence of *ATH1* in the SAM under all light conditions, inhibiting RZ activity, with the characteristic compact rosette of Arabidopsis as result. In line with this, loss of rosette compactness has been observed in light-grown Arabidopsis plants lacking multiple functional phytochrome and/or cryptochrome photoreceptors. Control of vegetative internode elongation in response to changes in light quality and/or ambient temperature was shown to be mediated by concerted action of phyA, phyB, phyD, phyE, and/or CRY1, all of which we identified as having a role in light-mediated induction of *ATH1* (Devlin *et al.*, 1996, 1998, 1999, 2003; Whitelam & Devlin, 1997; Whitelam *et al.*, 1998; Mazzella *et al.*, 2000; Franklin *et al.*, 2003; Kanyuka *et al.*, 2003; Strasser *et al.*, 2010; Zhang *et al.*, 2017). Often not appreciated in the literature, compact rosette habit is thus a genuine photomorphogenic trait in Arabidopsis. Remarkably, rosette internode compactness is a non-plastic trait, unlike other photoreceptor-driven developmental responses in Arabidopsis, such as elongation of hypocotyl, petiole, and inflorescence stem. Compact rosette growth is not affected in wild-type plants even under light quality and/or temperature regimes that cause rapid elongation of aerial plant organs. Plasticity of growth and development is often considered adaptive, enabling sessile plants to adjust rapidly to a changing environment (Schlichting, 1986; Schlichting & Levin, 1986). However, as mentioned, rosette growth provides several advantages compared with caulescent growth. Loss of a compact rosette in response to environmental cues, therefore, might be detrimental to plant fitness and viability. Compact rosette habit is not constitutively expressed in all rosette species (our unpublished observations) and this trait, as a result of selection, may have become fixed in Arabidopsis through genetic assimilation (Ehrenreich & Pfennig, 2016). Important contributors to genetic assimilation are genetic variants that alter gene regulation. Plausible ways in which gene regulation might facilitate loss of phenotypic plasticity are (i) decoupling of the regulation of genes that control a plastic trait from environmental cues or (ii) the evolution of additional regulatory pathways that makes their expression insensitive to the environment (Ehrenreich & Pfennig, 2016). The latter might be the case for Arabidopsis rosette internodes, given that *ATH1* expression is induced in response to broad wavelengths involving multiple photoreceptors. Moreover, it has been proposed that ATH1 controls internode elongation by antagonizing a large number of genes that promote internode growth, mostly independent of each other (Ejaz *et al.*, 2021). This assumption fits with the observation that *pifq* not completely reduced internode elongation in *ath1-3*. Such multitarget control by ATH1 of genes that affect internode elongation would further contribute to the robustness of compact rosette habit in Arabidopsis. Therefore, it is of interest to investigate whether ATH1 has a similar role in other rosette species and, if so, whether differences in plasticity of rosette compactness can be linked to differences in light-signaling control of *ATH1* and/or decoupling internode elongation genes from ATH1 regulation.

In this study, we identified *PIF1*, *PIF3*, *PIF4*, and *PIF5* as transcriptional targets of ATH1. *PIF4* and PIF signaling components were previously identified as binding target of ATH1 (Ejaz *et al.*, 2021). Therefore, ATH1 might affect the expression of these four *PIF* genes through direct transcriptional repression. Our finding that PIF4, and at least one of the other PIF proteins, PIF1, PIF3, or PIF5, in turn function as negative regulators of *ATH1* suggest the presence of a double-negative feedback loop between ATH1 and PIF family members (Fig. 7). Whether these PIFs also directly target *ATH1* is currently unknown, but, given the fact that the rib-zone expressed cytokinin catabolism gene *CKX5* is a direct transcriptional target of these PIFs (Hornitschek *et al.*, 2012; Zhang *et al.*, 2013; Pfeiffer *et al.*, 2016) and *ATH1*-promoter activity is strongly induced by cytokinin, we hypothesize that the PIF inhibitory effect on *ATH1* is indirect, via local reduction in cytokinin levels.

Signaling systems that contain double-negative feedback loops can, in principle, convert graded inputs into switch-like, irreversible responses (Ferrell, 2002). Such a genetic toggle switch is a bistable dynamical system, possessing two stable equilibria, each associated to a fully expressed protein. ATH1 has a fundamental role in maintaining internode compactness in Arabidopsis during vegetative

growth. In light-grown plants, *ATH1* is expressed throughout the shoot meristem, including the subapical region where it represses stem growth. Plant switching to reproductive growth rapidly down-regulate *ATH1* at the shoot meristem, marking the onset of bolting and emergence of an elongated inflorescence (Proveniers *et al.*, 2007; Gómez-Mena & Sablowski, 2008; Ejaz *et al.*, 2021). Such stem elongation is absent in plants constitutively expressing *ATH1*, without affecting flower formation (Cole *et al.*, 2006; Gómez-Mena & Sablowski, 2008; Rutjens *et al.*, 2009). Present study shows that both absence of ATH1 and induced *ATH1* expression leads to pronounced changes in *PIF* gene expression at the SAM associated with significant elongation or complete suppression of rosette internodes, respectively. PIF proteins have been associated with bolting time and/or stem internode elongation (Brock *et al.*, 2010; Todaka *et al.*, 2012; Galvão *et al.*, 2019; Arya *et al.*, 2021; Jenkitkonchai *et al.*, 2021). Moreover, elongated rosette internodes can be observed in *35S::PIF4* plants (Fig. 1d in Kumar *et al.* (2012)). It is therefore proposed that an ATH1-PIF toggle switch underlies the rapid and distinctive switch in Arabidopsis growth habit that marks floral transition.

Acknowledgements

phyA cry1, *phyB cry1* and *phyA phyB cry1* seeds were a kind gift of Jorge Casal. *hy1*, *cry1*, *cry2*, *cry1 cry2*, *hy1 cry1*, *hy1 cry2*, and *hy1 cry1 cry2* seeds were a kind gift of Enrique Lopez-Juez and *cop1-4* seeds were kind gift of Jan Lohmann. This work was supported by the Dutch Resource Council (NWO): ALW Graduate School grant 831.13.004 (SSS).

Competing interests

None declared.

Author contributions

MP was involved in conceptualization. MP, SSH, SSS and ES were involved in methodology. SSH, ES, NP, GB and SSS were involved in investigation. MP and SSH were involved in writing–original draft. MP, SSH, SSS, ES and SS were involved in writing–review and editing. MP, SSS, SSH and SS were involved in funding acquisition. SSH was involved in visualization. MP, ES and SS were involved in resources. MP and SS were involved in supervision.

ORCID

Marcel Proveniers https://orcid.org/0000-0001-7896-6049
Shahram Shokrian Hajibehzad https://orcid.org/0000-0002-3338-4472
Sjef Smeekens https://orcid.org/0000-0001-6631-9426

Data availability

All data supporting the findings are contained in this manuscript. Additional Supporting Information may be found in the Supporting Information section at the end of the article.

References

Araki T, Komeda Y. 1993. Flowering in darkness in *Arabidopsis thaliana*. *The Plant Journal* **4**: 801–811.

Arya H, Singh MB, Bhalla PL. 2021. Overexpression of PIF4 affects plant morphology and accelerates reproductive phase transitions in soybean. *Food and Energy Security* **10**: e291.

Bello FD, Lepš J, Sebastià M-T. 2005. Predictive value of plant traits to grazing along a climatic gradient in the Mediterranean. *Journal of Applied Ecology* **42**: 824–833.

Bencivenga S, Serrano-Mislata A, Bush M, Fox S, Sablowski R. 2016. Control of oriented tissue growth through repression of organ boundary genes promotes stem morphogenesis. *Developmental Cell* **39**: 198–208.

Brock MT, Maloof JN, Weinig C. 2010. Genes underlying quantitative variation in ecologically important traits: PIF4 (PHYTOCHROME INTERACTING FACTOR 4) is associated with variation in internode length, flowering time, and fruit set in *Arabidopsis thaliana*. *Molecular Ecology* **19**: 1187–1199.

Cai W, Li X, Liu Y, Wang Y, Zhou Y, Xu T, Xiong Y. 2017. COP1 integrates light signals to ROP2 for cell cycle activation. *Plant Signaling & Behavior* **12**: e1363946.

Chen G-H, Liu M-J, Xiong Y, Sheen J, Wu S-H. 2018. TOR and RPS6 transmit light signals to enhance protein translation in deetiolating Arabidopsis seedlings. *Proceedings of the National Academy of Sciences, USA* **115**: 828.

Chen M, Chory J. 2011. Phytochrome signaling mechanisms and the control of plant development. *Trends in Cell Biology* **21**: 664–671.

Chourey PS, Li Q-B, Kumar D. 2010. Sugar–hormone cross-talk in seed development: two redundant pathways of IAA biosynthesis are regulated differentially in the invertase-deficient miniature1 (mn1) seed mutant in maize. *Molecular Plant* **3**: 1026–1036.

Cole M, Nolte C, Werr W. 2006. Nuclear import of the transcription factor SHOOT MERISTEMLESS depends on heterodimerization with BLH proteins expressed in discrete sub-domains of the shoot apical meristem of *Arabidopsis thaliana*. *Nucleic Acids Research* **34**: 1281–1292.

Deng X, Quail PH. 1992. Genetic and phenotypic characterization of cop1 mutants of *Arabidopsis thaliana*. *The Plant Journal* **2**: 83–95.

Deprost D, Yao L, Sormani R, Moreau M, Leterreux G, Nicolaï M, Bedu M, Robaglia C, Meyer C. 2007. The Arabidopsis TOR kinase links plant growth, yield, stress resistance and mRNA translation. *EMBO Reports* **8**: 864–870.

Devlin PF, Halliday KJ, Harberd NP, Whitelam GC. 1996. The rosette habit of *Arabidopsis thaliana* is dependent upon phytochrome action: novel phytochromes control internode elongation and flowering time. *The Plant Journal* **10**: 1127–1134.

Devlin PF, Patel SR, Whitelam GC. 1998. Phytochrome E influences internode elongation and flowering time in Arabidopsis. *The Plant Cell* **10**: 1479–1487.

Devlin PF, Robson PRH, Patel SR, Goosey L, Sharrock RA, Whitelam GC. 1999. Phytochrome D acts in the shade-avoidance syndrome in Arabidopsis by controlling elongation growth and flowering time. *Plant Physiology* **119**: 909–916.

Devlin PF, Yanovsky MJ, Kay SA. 2003. A genomic analysis of the shade avoidance response in Arabidopsis. *Plant Physiology* **133**: 1617–1629.

Dong P, Xiong F, Que Y, Wang K, Yu L, Li Z, Ren M. 2015. Expression profiling and functional analysis reveals that TOR is a key player in regulating photosynthesis and phytohormone signaling pathways in Arabidopsis. *Frontiers in Plant Science* **6**: 677.

Ehrenreich IM, Pfennig DW. 2016. Genetic assimilation: a review of its potential proximate causes and evolutionary consequences. *Annals of Botany* **117**: 769–779.

Ejaz M, Bencivenga S, Tavares R, Bush M, Sablowski R. 2021. *ARABIDOPSIS THALIANA* HOMEOBOX GENE 1 controls plant architecture by locally restricting environmental responses. *Proceedings of the National Academy of Sciences, USA* **118**: e2018615118.

Ferrell JE. 2002. Self-perpetuating states in signal transduction: positive feedback, double-negative feedback and bistability. *Current Opinion in Cell Biology* **14**: 140–148.

Franklin KA, Praekelt U, Stoddart WM, Billingham OE, Halliday KJ, Whitelam GC. 2003. Phytochromes B, D, and E act redundantly to control

multiple physiological responses in Arabidopsis. *Plant Physiology* **131**: 1340–1346.

Fujita N, Koda R. 2015. Capitulum and rosette leaf avoidance from grazing by large herbivores in Taraxacum. *Ecological Research* **30**: 517–525.

Galvão VC, Fiorucci A-S, Trevisan M, Franco-Zorilla JM, Goyal A, Schmid-Siegert E, Solano R, Fankhauser C. 2019. PIF transcription factors link a neighbor threat cue to accelerated reproduction in Arabidopsis. *Nature Communications* **10**: 4005.

Gómez-Mena C, Sablowski R. 2008. *ARABIDOPSIS THALIANA* HOMEOBOX GENE1 establishes the basal boundaries of shoot organs and controls stem growth. *The Plant Cell* **20**: 2059–2072.

Hornitschek P, Kohnen MV, Lorrain S, Rougemont J, Ljung K, López-Vidriero I, Franco-Zorrilla JM, Solano R, Trevisan M, Pradervand S *et al.* 2012. Phytochrome interacting factors 4 and 5 control seedling growth in changing light conditions by directly controlling auxin signaling. *The Plant Journal* **71**: 699–711.

Hu Q, Merchante C, Stepanova AN, Alonso JM, Heber S. 2016. Genome-wide search for translated upstream open reading frames in *Arabidopsis Thaliana*. *IEEE Transactions on NanoBioscience* **15**: 150–159.

Hu W, Franklin KA, Sharrock RA, Jones MA, Harmer SL, Lagarias JC. 2013. Unanticipated regulatory roles for Arabidopsis phytochromes revealed by null mutant analysis. *Proceedings of the National Academy of Sciences, USA* **110**: 1542–1547.

Jacqmard A, Gadisseur I, Bernier G. 2003. Cell division and morphological changes in the shoot apex of *Arabidopsis thaliana* during floral transition. *Annals of Botany* **91**: 571–576.

Janocha D, Pfeiffer A, Dong Y, Novák O, Strnad M, Ryabova LA, Lohmann JU. 2021. TOR kinase controls shoot development by translational regulation of cytokinin catabolic enzymes. *BioRxiv*. doi: 10.1101/2021.07.29.454319.

Jenkitkonchai J, Marriott P, Yang W, Sriden N, Jung J, Wigge PA, Charoensawan V. 2021. Exploring PIF4's contribution to early flowering in plants under daily variable temperature and its tissue-specific flowering gene network. *Plant Direct* **5**: e339.

Kanyuka K, Praekelt U, Franklin KA, Billingham OE, Hooley R, Whitelam GC, Halliday KJ. 2003. Mutations in the huge Arabidopsis gene BIG affect a range of hormone and light responses. *The Plant Journal* **35**: 57–70.

Kathare PK, Xu X, Nguyen A, Huq E. 2020. A COP1-PIF-HEC regulatory module fine-tunes photomorphogenesis in Arabidopsis. *The Plant Journal* **104**: 113–123.

Kumar SV, Lucyshyn D, Jaeger KE, Alós E, Alvey E, Harberd NP, Wigge PA. 2012. Transcription factor PIF4 controls the thermosensory activation of flowering. *Nature* **484**: 242–245.

Kurihara D, Mizuta Y, Sato Y, Higashiyama T. 2015. ClearSee: a rapid optical clearing reagent for whole-plant fluorescence imaging. *Development* **142**: 4168–4179.

Larcher W, Kainmüller C, Wagner J. 2010. Survival types of high mountain plants under extreme temperatures. *Flora–Morphology, Distribution, Functional Ecology of Plants* **205**: 3–18.

LeClere S, Schmelz EA, Chourey PS. 2010. Sugar levels regulate tryptophan-dependent auxin biosynthesis in developing maize kernels. *Plant Physiology* **153**: 306–318.

Leivar P, Tepperman JM, Monte E, Calderon RH, Liu TL, Quail PH. 2009. Definition of early transcriptional circuitry involved in light-induced reversal of PIF-imposed repression of photomorphogenesis in young Arabidopsis seedlings. *The Plant Cell* **21**: 3535–3553.

Li L, Sheen J. 2016. Dynamic and diverse sugar signaling. *Current Opinion in Plant Biology* **33**: 116–125.

Li X, Cai W, Liu Y, Li H, Fu L, Liu Z, Xu L, Liu H, Xu T, Xiong Y. 2017. Differential TOR activation and cell proliferation in Arabidopsis root and shoot apexes. *Proceedings of the National Academy of Sciences, USA* **114**: 2765–2770.

Li Y, Pi L, Huang H, Xu L. 2012. ATH1 and KNAT2 proteins act together in regulation of plant inflorescence architecture. *Journal of Experimental Botany* **63**: 1423–1433.

Livak KJ, Schmittgen TD. 2001. Analysis of relative gene expression data using real-time quantitative PCR and the $2^{-\Delta\Delta CT}$ method. *Methods* **25**: 402–408.

López-Juez E, Dillon E, Magyar Z, Khan S, Hazeldine S, Jager SM, Murray JAH, Beemster GTS, Bögre L, Shanahan H. 2008. Distinct light-initiated gene expression and cell cycle programs in the shoot apex and cotyledons of Arabidopsis. *The Plant Cell* **20**: 947–968.

Ma D, Li X, Guo Y, Chu J, Fang S, Yan C, Noel JP, Liu H. 2016. Cryptochrome 1 interacts with PIF4 to regulate high temperature-mediated hypocotyl elongation in response to blue light. *Proceedings of the National Academy of Sciences, USA* **113**: 224–229.

Mazzella MA, Bertero D, Casal JJ. 2000. Temperature-dependent internode elongation in vegetative plants of *Arabidopsis thaliana* lacking phytochrome B and cryptochrome 1. *Planta* **210**: 497–501.

de Mendiburu F. 2021. *Statistical procedures for agricultural research. Package 'agricolae' (v.1.3-5)*. [WWW document] URL https://cran.r-project.org/web/packages/agricolae/index.html [accessed 3 February 2023].

Mohammed B, Bilooei SF, Dóczi R, Grove E, Railo S, Palme K, Ditengou FA, Bögre L, López-Juez E. 2017. Converging light, energy and hormonal signaling control meristem activity, leaf initiation, and growth. *Plant Physiology* **176**: 1365–1381.

Montané M-H, Menand B. 2013. ATP-competitive mTOR kinase inhibitors delay plant growth by triggering early differentiation of meristematic cells but no developmental patterning change. *Journal of Experimental Botany* **64**: 4361–4374.

Pedmale UV, Huang SC, Zander M, Cole BJ, Hetzel J, Ljung K, Reis PAB, Sridevi P, Nito K, Nery JR *et al.* 2016. Cryptochromes interact directly with pifs to control plant growth in limiting blue light. *Cell* **164**: 233–245.

Peterson RL, Yeung EC. 1972. Effect of two gibberellins on species of the rosette plant hieracium. *Botanical Gazette* **133**: 190–198.

Pfeiffer A, Janocha D, Dong Y, Medzihradszky A, Schöne S, Daum G, Suzaki T, Forner J, Langenecker T, Rempel E *et al.* 2016. Integration of light and metabolic signals for stem cell activation at the shoot apical meristem. *eLife* **5**: e17023.

Pham VN, Kathare PK, Huq E. 2018a. Dynamic regulation of PIF5 by COP1–SPA complex to optimize photomorphogenesis in Arabidopsis. *The Plant Journal* **96**: 260–273.

Pham VN, Kathare PK, Huq E. 2018b. Phytochromes and phytochrome interacting factors. *Plant Physiology* **176**: 1025–1038.

Pham VN, Xu X, Huq E. 2018c. Molecular bases for the constitutive photomorphogenic phenotypes in Arabidopsis. *Development* **145**: dev169870.

Ponnu J, Hoecker U. 2021. Illuminating the COP1/SPA ubiquitin ligase: fresh insights into its structure and functions during plant photomorphogenesis. *Frontiers in Plant Science* **12**: 662793.

Proveniers M, Rutjens B, Brand M, Smeekens S. 2007. The Arabidopsis TALE homeobox gene ATH1 controls floral competency through positive regulation of FLC. *The Plant Journal* **52**: 899–913.

Quaedvlieg N, Dockx J, Rook F, Weisbeek P, Smeekens S. 1995. The homeobox gene ATH1 of Arabidopsis is derepressed in the photomorphogenic mutants cop1 and det1. *The Plant Cell* **7**: 117–129.

Rabot A, Henry C, Baaziz KB, Mortreau E, Azri W, Lothier J, Hamama L, Boummaza R, Leduc N, Pelleschi-Travier S *et al.* 2012. Insight into the role of sugars in bud burst under light in the rose. *Plant and Cell Physiology* **53**: 1068–1082.

Ramon M, Rolland F, Sheen J. 2008. Sugar sensing and signaling. *The Arabidopsis Book* **6**: e0117.

Roldán M, Gómez-Mena C, Ruiz-García L, Salinas J, Martínez-Zapater JM. 1999. Sucrose availability on the aerial part of the plant promotes morphogenesis and flowering of Arabidopsis in the dark. *The Plant Journal* **20**: 581–590.

Rutjens B, Bao D, Eck-Stouten EV, Brand M, Smeekens S, Proveniers M. 2009. Shoot apical meristem function in Arabidopsis requires the combined activities of three BEL1-like homeodomain proteins. *The Plant Journal* **58**: 641–654.

Sachs RM, Bretz CF, Lang A. 1959. Shoot histogenesis: the early effects of gibberellin upon stem elongation in two rosette plants. *American Journal of Botany* **46**: 376–384.

Sairanen I, Novák O, Pěnčík A, Ikeda Y, Jones B, Sandberg G, Ljung K. 2012. Soluble carbohydrates regulate auxin biosynthesis via PIF proteins in Arabidopsis. *The Plant Cell* **24**: 4907–4916.

Schaffer WM, Schaffer MV. 1979. The adaptive significance of variations in reproductive habit in the Agavaceae II: pollinator foraging behavior and selection for increased reproductive expenditure. *Ecology* **60**: 1051–1069.

Schepetilnikov M, Dimitrova M, Mancera-Martínez E, Geldreich A, Keller M, Ryabova LA. 2013. TOR and S6K1 promote translation reinitiation of uORF-containing mRNAs via phosphorylation of eIF3h. *The EMBO Journal* **32**: 1087–1102.

Schepetilnikov M, Kobayashi K, Geldreich A, Caranta C, Robaglia C, Keller M, Ryabova LA. 2011. Viral factor TAV recruits TOR/S6K1 signalling to activate reinitiation after long ORF translation. *The EMBO Journal* **30**: 1343–1356.

Schepetilnikov M, Makarian J, Srour O, Geldreich A, Yang Z, Chicher J, Hammann P, Ryabova LA. 2017. GTPase ROP2 binds and promotes activation of target of rapamycin, TOR, in response to auxin. *The EMBO Journal* **36**: 886–903.

Schepetilnikov M, Ryabova LA. 2017. Recent discoveries on the role of TOR (target of rapamycin) signaling in translation in plants. *Plant Physiology* **176**: 1095–1105.

Schlichting CD, Levin DA. 1986. Phenotypic plasticity: an evolving plant character. *Biological Journal of the Linnean Society* **29**: 37–47.

Schlichting CD. 1986. The evolution of phenotypic plasticity in plants. *Annual Review of Ecology and Systematics* **17**: 667–693.

Schneider CA, Rasband WS, Eliceiri KW. 2012. NIH Image to ImageJ: 25 y of image analysis. *Nature Methods* **9**: 671–675.

Serrano-Mislata A, Bencivenga S, Bush M, Schiessl K, Boden S, Sablowski R. 2017. DELLA genes restrict inflorescence meristem function independently of plant height. *Nature Plants* **3**: 749–754.

Strasser B, Sánchez-Lamas M, Yanovsky MJ, Casal JJ, Cerdán PD. 2010. *Arabidopsis thaliana* life without phytochromes. *Proceedings of the National Academy of Sciences, USA* **107**: 4776–4781.

Thomson FJ, Moles AT, Auld TD, Kingsford RT. 2011. Seed dispersal distance is more strongly correlated with plant height than with seed mass. *Journal of Ecology* **99**: 1299–1307.

Todaka D, Nakashima K, Maruyama K, Kidokoro S, Osakabe Y, Ito Y, Matsukura S, Fujita Y, Yoshiwara K, Ohme-Takagi M *et al.* 2012. Rice phytochrome-interacting factor-like protein OsPIL1 functions as a key regulator of internode elongation and induces a morphological response to drought stress. *Proceedings of the National Academy of Sciences, USA* **109**: 952.

Ursache R, Andersen TG, Marhavý P, Geldner N. 2018. A protocol for combining fluorescent proteins with histological stains for diverse cell wall components. *The Plant Journal* **93**: 399–412.

Vaughan JG. 1955. The morphology and growth of the vegetative and reproductive apices of *Arabidopsis thaliana* (L.) Heynh., *Capsella bursa-pastoris* (L.) Medic. and *Anagallis arvensis* L. *Journal of the Linnean Society of London, Botany* **55**: 279–301.

Whitelam GC, Devlin PF. 1997. Roles of different phytochromes in Arabidopsis photomorphogenesis. *Plant, Cell & Enviroment* **20**: 752–758.

Whitelam GC, Patel S, Devlin PF. 1998. Phytochromes and photomorphogenesis in Arabidopsis. *Philosophical Transactions of the Royal Society of London. Series B: Biological Sciences* **353**: 1445–1453.

Xiong Y, McCormack M, Li L, Hall Q, Xiang C, Sheen J. 2013. Glucose–TOR signalling reprograms the transcriptome and activates meristems. *Nature* **496**: 181–186.

Xu X, Paik I, Zhu L, Bu Q, Huang X, Deng XW, Huq E. 2014. PHYTOCHROME INTERACTING FACTOR1 Enhances the E3 Ligase Activity of CONSTITUTIVE PHOTOMORPHOGENIC1 to synergistically repress photomorphogenesis in Arabidopsis. *The Plant Cell* **26**: 1992–2006.

Zhang B, Holmlund M, Lorrain S, Norberg M, Bakó L, Fankhauser C, Nilsson O. 2017. BLADE-ON-PETIOLE proteins act in an E3 ubiquitin ligase complex to regulate PHYTOCHROME INTERACTING FACTOR 4 abundance. *eLife* **6**: e26759.

Zhang Y, Mayba O, Pfeiffer A, Shi H, Tepperman JM, Speed TP, Quail PH. 2013. A quartet of PIF bHLH factors provides a transcriptionally centered signaling hub that regulates seedling morphogenesis through differential expression-patterning of shared target genes in Arabidopsis. *PLoS Genetics* **9**: e1003244.

Supporting Information

Additional Supporting Information may be found online in the Supporting Information section at the end of the article.

Fig. S1 Different *ath1* alleles display highly comparable rosette internode phenotypes.

Fig. S2 *GUS* mRNA levels in sucrose-induced $ATH1_{pro}$:*GUS* seedlings.

Fig. S3 Sugar-induced, dark-grown *Arabidopsis thaliana* seedlings phenocopy light-grown *ath1*mutants.

Fig. S4 Relative *ATH1* mRNA abundance in different *Arabidopsis thaliana* photoreceptor mutants.

Fig. S5 $ATH1_{pro}$:*GUS* activity in dark-grown *Arabidopsis thaliana* seedlings in the presence of different sugars.

Fig. S6 Chemical inhibition of photosynthesis negatively impacts *ATH1*-promoter activity.

Fig. S7 Effect of TOR kinase activity on *ATH1*-promoter activity.

Fig. S8 Sugar-mediated dark morphogenesis requires TOR kinase activity.

Fig. S9 Effect of TOR inhibition on *ATH1* expression in *cop1-4* mutant seedlings.

Fig. S10 Cytokinin potently induces *ATH1*-promoter activity in the absence of both light and sucrose.

Table S1 Arabidopsis thaliana genotypes used in this study.

Table S2 PCR primers used for genotyping.

Table S3 Primers used for qPCR.

Please note: Wiley is not responsible for the content or functionality of any Supporting Information supplied by the authors. Any queries (other than missing material) should be directed to the *New Phytologist* Central Office.